

Slutrapport

Energimyndighetens titel på projektet – svenska

Framställning, struktur och tillämpning av bio-bindemedel för elektroder och eldfastamaterial inom metallurgisk processindustri

Energimyndighetens titel på projektet – engelska

Synthesis, Structure and Application of Bio-Binders for Electrodes and Refractories in the Metallurgical Process Industries

Organisation

Kungliga Tekniska Högskolan

Department of Materials Science and Engineering

Brinellvägen 23, 100 44 Stockholm

Nyckelord

Carbon electrodes; Söderberg electrode paste; Anodes and cathodes aluminum smelting; Carbon refractories; Biocarbon in electrodes; Catalytic graphitization

Förord

Myndighet: Energimyndigheten

Utlysning: Bioplus 2022 FoI – Vill du bidra med kunskap om biomassans roll i samhället och hållbara biobaserade lösningar?

Delområde: Biomassa och biobaserade lösningar

Partners: BTG Bioliquids, Elkem Carbon Solutions, INTOCAST

2026-02-04

2026-201629-0001

2026-201629-0001 2026-02-04

Innehållsförteckning

Sammanfattning	4
Summary	4
Inledning/bakgrund	5
Genomförande	10
Resultat	11
Diskussion	12
Publikationslista	63
Referenser, källor	64
Bilagor	70

Sammanfattning

Kol är ett kritiskt material i många metallurgiska industrisektorer, och inte bara som ett reduktionsmedel. Koles unika kemiska och strukturella mångsidighet samt termofysiska egenskaper gör det i princip oersättligt i ugnselektroder och kolinnehållande eldfastamaterial. Det finns alltså en betydande drivkraft för att hitta kolkomponenter av biologiskt ursprung för ersättning av fossila kolmaterial som för närvarande används i dessa kolförnödenheter. Detta projekt syftar till att vidareutveckla tekniskt genomförbara biobaserade kolbindemedel för användning vid tillverkning av kolelektroder, stampemasser och kolhaltiga oxideldfasta material som är så kritiska för stål- och icke-järnmetallindustrin.

Summary

Carbon is a critical material in several metallurgical industrial sectors, and not just as a reducing agent. The unique chemical and structural versatility, and thermo-physical properties of carbon make it essentially irreplaceable in furnace electrodes and carbon containing refractories. Thus, there is considerable driving force to find viable bioderived substitutes for fossil carbon materials currently used in these carbon consumables. This project aims to further develop technically viable bio-carbon binders towards application in the manufacture of carbon electrodes, carbon lining pastes, and carbon-containing oxide refractories so critical to the steel and non-ferrous metal industries.

Inledning/bakgrund

Background

Heavy pressure is on the metallurgical industries to phase out fossil carbon usage. However, fossil carbon materials in many forms are vital to the metallurgical industries. A major transition is currently underway to replace or partially substitute fossil carbon as a reductant, for example by using hydrogen, or by partially or fully substituting it with biomass or charcoal.

Due to its unique combination of properties, carbon is employed as both a refractory material (resistant to both heat and chemical corrosion), and as an electrical and thermal conductor in refractory furnace linings and for electrodes. Replacing carbon in these applications presents a major materials-engineering challenge, as no alternative material currently offers the same performance across all required functions.

Natural graphite is a scarce mined resource and has been listed as a critical raw material (CRM) vital to the European economies [1]. China currently holds a near monopoly on the global graphite market, as most of the major graphite mines are located within its territory. Sweden has strong potential to become a pioneer in the extraction, production, and distribution of graphite in Europe [2], owing to its natural graphite resources and renewable precursors for graphitizable materials derived from its well-established mining, forestry, and paper industries. These resources can support the development of domestic graphite supply chains for metallurgical and refractory applications, where high-quality carbon materials are essential. Such industries make extensive use of carbon-based materials that, although not always graphite in their original form, can be readily graphitized to a certain extent.

Carbon materials can be broadly classified into graphitizable carbons and non-graphitizable carbons. These are commonly referred to as “soft” and “hard” carbon materials, respectively. Soft carbon materials are readily graphitized by simple heat treatment up to 3000°C, and the thermophysical properties of the bulk polycrystalline material approach that of a single crystal of graphite [3]. The availability of high-quality fossil carbon materials is declining globally. Most petroleum pitches and cokes, coking coals, and coal tar pitches (CTP) are soft carbons that are readily graphitizable. Low-sulphur petroleum coke is becoming increasingly scarce and must be imported to Europe.

Coal tar pitch is the binder of excellence for carbon electrode materials. It is highly aromatic, thermally stable, and produces high coking residue during electrode baking. It also has a complex flow behavior that makes it perfectly suitable for creating dense, homogenous and strong carbon electrodes [4]. Despite these favorable characteristics, CTP contains high concentrations of polycyclic aromatic hydrocarbons (PAH) of which some components are considered carcinogenic and

damaging for the environment. The usage of this binder has been limited by various legislations globally, namely REACH in the EU and K-Reach in Korea with an aim of phasing out/further limiting this use in the coming future [5]. The supply issues and the increased awareness about the need to reduce the carbon-footprint of the carbon electrode materials are driving forces to look for renewable and environmentally friendly binders.

Carbon materials are heavily relied upon in both ironmaking and secondary steelmaking in refractories and electrodes. Graphite blocks are employed in blast furnace hearths. Carbon-containing refractories such as magnesia carbon (MgO–C) are in prevalent use in converters and ladle linings. In secondary, scrap-based steelmaking, large electric arc furnaces consume enormous quantities of graphite electrodes.

In primary aluminium production, alumina is reduced in high-temperature Hall-Héroult electrolytic cells. Carbon anodes and cathodes in the cells generate the Joule heating as well as electrical current and carbon for reduction. While the cathodes last the lifetime of the cell (> 5 years), the anodes are continuously consumed in the process as oxygen released by electrolysis reacts with anodes to generate CO₂ gas. Efforts have been made for decades to develop inert anodes in aluminum electrolysis but so far without commercial success [6].

In silicon and ferroalloy production, large electric submerged-arc furnaces are employed using carbon Söderberg electrodes. The primary role of the electrodes in these processes is to supply Joule heat to the furnace (most of the reductant carbon is contained in the charge). The key principle of operation in a Söderberg electrode system, involves the shaping and baking of the carbon paste occurring in-situ in a continuous process within the electrode column [7]. These electrodes were patented by C.W. Söderberg in 1919 at Elkem's Fiskaa Verk (in Kristiansand, Norway), but their use is still prevalent today, with electrode diameters reaching 2 m in modern furnaces. **Figure 1** shows schematic representation of Söderberg electrode. A cylindrical steel casing is continuously filled with paste (made of anthracite aggregates and binder), which softens and flows into a compact block, filling the casing and all spaces between the fins of the casing, then bakes as the electrode slips through the contact shoes and experiences temperatures upward of 500 °C, transforming the paste into a mechanically sound, electrically conductive carbon electrode [8]. Furthermore, the furnace linings in silicon and ferroalloy furnaces are partially constructed of either carbon blocks or carbon lining paste.

Carbon electrodes of all types (this includes Söderberg, prebaked, and anodes and cathodes for Al), and carbon ramming and lining pastes are similar in that they are composite materials comprised of a granular carbon aggregate together with a carbon-based binder. Traditional Söderberg electrode paste is composed of 70–80% carbon aggregate, and 20–30% coal tar pitch binder [9]. A typical pre-baked anode in Al production contains about 65% calcined petroleum coke, 20% recycled anode butts, and 15% coal tar pitch binder [10]. Refractories like MgO–C typically

2026-201629-0001 2026-02-04

contain 12–20% flake (natural) graphite, and 5% petroleum-derived phenolic resin binder [11].

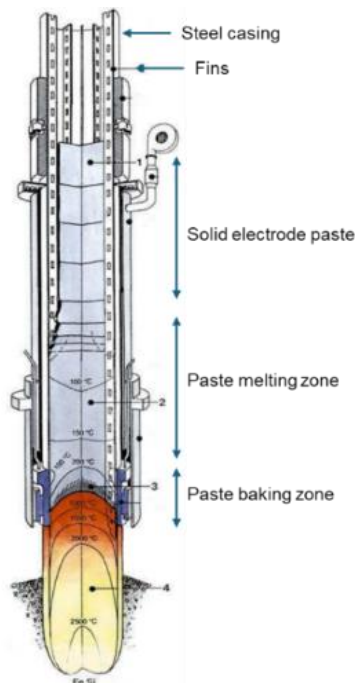


Figure 1. Illustration of a Söderberg electrode, courtesy of Elkem Carbon.

Motivation

Carbon is irreplaceable for non-reducing applications in many high-temperature metallurgical processes. Currently, bio-carbon substitutes are not technically viable for use in electrode and refractory materials. This project aims to develop technical pathways to address these limitations.

Charcoal, as a substitute for fossil carbon aggregates in carbon electrodes (outside of Söderberg electrodes), is technically feasible only up to about ten percent [12]. Being a hard carbon, charcoal exhibits low electrical conductivity even after thermal treatment, which currently prevents its use in graphite electrodes for steelmaking, where high current densities are required. Furthermore, alkali and alkaline earth metals in the ash catalyze so-called “reactivity” with oxygen and CO₂ [13]. Catalytic graphitization of charcoal using iron could be a potential approach to convert charcoal into a material suitable for electrode and refractory applications [14], though significant technical challenges remain, such as efficient catalyst separation. Another possible approach could be the graphitization of lignin by-products to produce solid carbon aggregate [15].

Replacing fossil-derived binders with bio-binders in carbon electrodes and refractory materials could dramatically reduce the carbon footprint of these products. Feasible biomass feedstocks for bio-binders include sawdust, wood chips, bark, black pulping liquor, lignin, liginosulphonates, and agricultural

residues [16]. Pioneering research has explored the production of bio-pitch suitable for carbon electrodes [17], and as of late for specific application in carbon anodes for aluminium electrolysis [18], [19], [20]. Laboratory-scale demonstrations of carbon anodes made with bio-pitch binders have been reported [21], although large-scale applications have yet to be realized. The aluminium industry is thus far leading the way, but bio-pitches derived from pyrolysis oils could also potentially be used in Söderberg electrode paste manufacture, lining and ramming pastes. While bio-pitch can be produced with favourable softening points and rheological properties for anode carbon electrodes, key difficulties to overcome are the high oxygen content, low coking value, and limited graphitizability [20], [21].

Implementation

The successful development of improved chemistries, process routes, and laboratory-scale demonstration of functional bio-binders for industrial use in electrodes and refractory materials would lay the foundation for scaling up production.

The next phase, beyond the scope of this project, would involve pilot-scale production of bio-binders in quantities sufficient for full-scale fabrication of carbon anodes, Söderberg electrodes, and magnesia-carbon refractories, followed by testing in actual industrial operations.

In the long term, commercial-scale production of bio-binders for these applications could enable the valorization of largely untapped biomass resources and by-products from the forestry and paper industries in Sweden and Scandinavia.

Not the least, replacing conventional binders with renewable bio-binders in carbon electrodes and refractories would substantially reduce the carbon footprint of these products, representing a major step toward enhancing the environmental sustainability of the metallurgical and steelmaking industries.

Overall and specific objectives

In summary, fossil carbon materials are particularly valuable for electrodes and refractories. These materials—including aggregates such as petroleum coke, anthracite, and natural flake graphite, along with binders like coal tar pitch and phenolic resins—possess unique properties that are difficult to replicate with biomass-derived carbon. Significant research and development are still needed to advance bio-carbon materials from the laboratory stage to practical applications in these demanding applications. Major challenges include high oxygen and alkali and alkaline earth metals contents, low coking value, and limited graphitizability. A clearly defined area of research with strong potential for rapid environmental impact is the development of highly functional bio-derived binders suitable for high-temperature applications.

Thus, the overall objective of this project is to develop bio-carbon binders that are technically feasible, commercially viable, and environmentally sustainable for use in the manufacture of carbon electrodes, carbon lining pastes, and carbon-containing refractories in the metallurgical industry.

Specific objectives

1. Determine optimal Swedish biomass feedstocks and improved chemistries and processing routes for bio-binders tailored for use in the respective high-temperature applications (TRL 2-3).
2. Simulation/measurement of structure and development of process routes to produce low reactivity, highly graphitizable bio-binders (TRL 2-3).
3. Investigate on the laboratory scale the performance of developed bio-binders in electrode and refractory materials in metallurgical processes, especially for carbon anodes for aluminium production, submerged arc electrodes used in silicon and ferroalloy production, and magnesia-carbon refractories employed in steelmaking (TRL 2-3).
4. Evaluate scale-up possibilities and economic analyses of bio-binder production and usage in the manufacture of carbon electrodes and refractories for metallurgical applications.
5. Disseminate project results by communicating with the steelmaking, aluminium, and silicon/ferroalloy, carbon materials and refractory industries at project meetings, conferences, and workshop

Genomförande

The work was mainly conducted by postdoctoral researcher Luis M. López-Renau guided by Faculty Affiliate Jesse F. White (KTH) and Full Professor Björn Glaser (KTH). A technical advisory board for the project was established with representatives from key industrial areas. Asem Hussein of Elkem Carbon Solutions is an expert in bio-pitches for carbon anodes. Hans Heeres of BTG Biomass Technology Group is an authority on biomass-derived products obtained from thermochemical conversion technologies. Roberto Caballero of Intocast is a recognized specialist in magnesia-carbon refractories.

The project comprised five work packages (WPs) and had a duration of 36 months (2022-11-01 to 2025-10-31). The total budget was 5 506 582 SEK. KTH was the project coordinator and majorly contributed to all the WPs. BTG provided biomass precursors and expertise in biomass material selection and processing in WP1 and WP2. WP1 and WP2 ran in parallel and in an iterative manner. Elkem Carbon Solutions provided expertise and technology for the manufacture of electrode bio-carbon pastes in WP3. All partners contributed to the techno-economic evaluation in the up-scaling of bio-based electrode pastes (WP4), as well as to project management and dissemination (WP5).

Work packages (WPs):

WP1: Optimal biomass feedstocks and processing for bio-binders for high-temperature applications (KTH, BTG)

- Evaluation of a range of feedstock materials from various Swedish sources
- Development of optimal thermochemical processing routes to obtain bio-binders with desirable physical and rheological properties for high-temperature applications
- Structural characterization of the structure, chemical composition, and physical properties of bio-binders

WP2: Structure and further processing routes for low reactivity, highly-graphitizable bio-binders (KTH, BTG)

- Development of optimal modification processes to obtain binder materials and precursors with low oxygen content and minimal harmful impurities
- Structural characterization and evaluation of the graphitization characteristics of refined bio-binders
- Based on the analysis of the results obtained, recommendations for process modifications in WP1 and WP2

2026-02-04

2026-201629-0001

WP3: Testing of bio-binders in electrode and refractory materials (Elkem, INTOCAST)

- Preparation of lab prototypes of carbon anode and Söderberg electrode materials by mixing aggregates with promising bio-binder materials
- Elaboration of a prototype recipe of a magnesia-carbon refractory material using bio-binders
- Testing of final products at relevant conditions

WP4: Report on evaluation of scale-up and economic analyses of bio-carbon electrodes and refractories for metallurgical applications (KTH, BTG, Elkem)

- Conceptual design of large-scale industrial processes for producing bio-binders in high volumes for use in electrode and refractory production
- Mass and energy balances, and development of process flow diagrams
- Economic analysis of large-scale bio-binder production based on optimal feedstocks

WP5: Project management and dissemination (KTH, BTG, Elkem)

- Overall responsibility of the project, including workflow, planning, and communications within and outside the project group
- Discussion of research progress with supervisors and group members through regular meetings

Resultat

Overview of Work Package discussion

This study evaluates the possibility of using solid pyrolytic lignin (SPL) (a bio-based binder) as a renewable alternative to coal-tar-pitch (CTP), the conventional binder for Söderberg electrode paste. SPL differs markedly from CTP in chemistry (higher oxygen content, lower aromaticity, low degree of crystallinity after baking), physical properties (higher softening point, lower coking value, lower density), and thermal behavior (earlier, multi-step decomposition). Despite an expected performance gap, laboratory electrodes produced with SPL—when processed within an adjusted window (lower mixing temperature, higher binder content, slower bake/slip rate during baking)—achieved comparable baked density, open porosity, air permeability, electrical resistivity, thermal conductivity, and equal or better oxidation resistance against air and CO₂. Overall, SPL could serve as a viable binder with process adaptations; however, its narrow processing window poses challenges not only for manufacturing but also for effective use in the electrode column, complicating its scale-up to industrial implementation.

1. Work package 1: Characterization of solid pyrolytic lignin

The present study investigates the potential of solid pyrolytic lignin (SPL) as a renewable binder for the production of bio-carbon electrodes in the metallurgical industry. SPL is obtained through the thermochemical fractionation (TCF) of lignocellulosic biomass, a process developed by BTG Biomass Technology Group. TCF separates fast pyrolysis bio-oil (FPBO) into two main streams: a water-diluted pyrolytic sugar fraction and liquid pyrolytic lignin, which can be further processed into solid lignin in the form of chunks or pastilles [22].

The bio-oil feedstock used to produce SPL in this study originates from the Pyrocell fast pyrolysis plant in Gävle, which converts 5 t/h of Swedish softwood sawdust into bio-oil for heating purposes. For the purpose of this work, FPBO was processed at BTG's pilot-scale facilities (TRL6/7, 120–125 kg/h) in the Netherlands for its fractionation into isolated sugars and lignin streams.

Pyrolytic lignin is characterized by a high content of high-molecular-weight, oxygenated aromatic compounds, derived from the three monomeric units of lignin: guaiacyl, syringyl, and p-hydroxyphenyl [23]. It typically exhibits a softening point between 90–110 °C and undergoes carbonization starting at 200 °C. Structurally, pyrolytic lignin has the potential to resemble graphite after catalytic graphitization, as defect elimination in the carbon network can lead to a highly organized, layered structure.

In this work, SPL is selected as a binder due to its renewable origin, aromatic composition, and favorable thermal behavior. Characterization of its chemical and

structural properties highlights Swedish-derived SPL as a viable and sustainable alternative to conventional fossil-based binders in carbon electrode manufacture.

For comparison, a benchmark coal tar pitch binder with a softening point of 90 °C, typically used in Söderberg electrode paste production at Elkem Carbon facilities, was selected. This industrial-grade CTP is characterized by high aromaticity, good thermal stability, and a high coking value, making it a suitable reference material for evaluating the performance of bio-based binders.

1.1. Characterization prior to carbonization

1.1.1. Chemical composition

Proximate and ultimate analyses of the binder samples were performed using thermogravimetric analysis (TGA) in air and CHNS elemental analysis, respectively, as presented in **Table 1**. The chemical groups in the binder pitches were qualitatively analyzed using a single-reflection attenuated total reflection (ATR) Fourier-Transform Infrared (FT-IR) system. The quinoline insoluble (QI) content was determined using a standard method, which involves digesting and filtering the binder samples in hot quinoline.

Table 1. Chemical composition of binder samples.

Sample	C (wt%)	H (wt%)	N (wt%)	S (wt%)	O (wt%)	Ash (wt%)	QI (wt%)
SPL	70.6	7.2	0.2	0.01	21.9	<0.1	0.9
CTP	91.0	4.5	1.2	0.52	2.9	~0.1	7.4

Binder samples have distinct origins, which explain the differences in their chemical composition. Coal tar pitch (CTP), on the one hand, is a fossil-based binder obtained through the vacuum flash distillation of coal tar. It consists of a wide variety of polycyclic aromatic hydrocarbons (PAHs), primarily composed of carbon and hydrogen, with minor amounts of nitrogen, sulfur, and oxygen impurities. The presence of PAHs is confirmed by FT-IR (see **Figure 2**) through aromatic C–H stretching vibrations (600–860 cm⁻¹) and aromatic and aliphatic C=C stretching vibrations (3000–3100 and 2940–2835 cm⁻¹, respectively) [18].

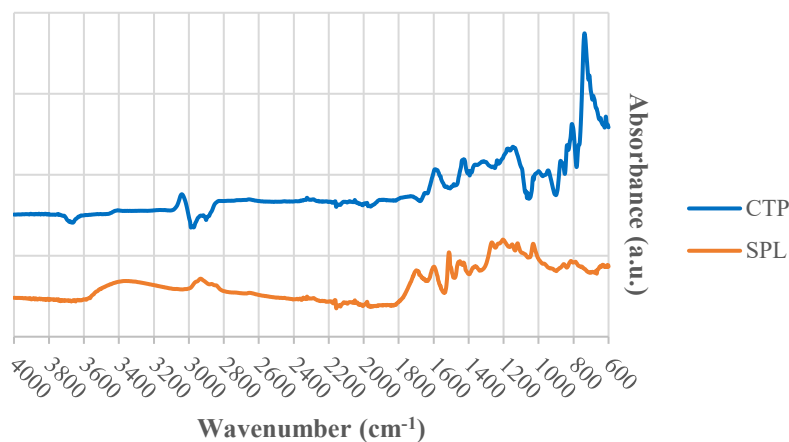


Figure 2. FT-IR spectra of binder samples.

Solid pyrolytic lignin (SPL), on the other hand, is obtained from the thermochemical fractionation of biomass. It consists of a wide variety of oxygenated phenolic structures derived from the (partly) depolymerization of lignin. In addition to the aliphatic and aromatic C–H and C=C bonds typically found in coal-tar pitch, SPL also contains oxygen-containing functional groups such as C–O and C=O (1200–1275 cm^{-1}), as well as –COOH and –OH groups (3100–3600 cm^{-1}) [18]. Consequently, this bio-based binder exhibits a substantially higher oxygen content than its fossil-derived counterpart. Since both binders originate from the condensation of vapors during distillation or pyrolysis, they exhibit low, or even negligible, ash contents.

The solubility of pitch samples in quinoline was determined by ISO 6791:1981 standard method. In this test pitch powder is dissolved in hot quinoline, then solution is filtered, and the residue is washed several times with hot quinoline. The percentage of residue is reported as the Quinoline Insoluble (QI). In CTP, the part that cannot be dissolved in hot quinoline (quinoline insoluble) is non-graphitizing, isotropic solid carbon particles which are formed by incomplete combustion of the tar vapors in the coke oven. The presence of the QI affects the microstructure of the carbonized CTP binder. These particles act as hard inclusions, that delay the formation of the mesophase spheres and prevent their growth and coalescence, and suppress long range graphitization, which is beneficial for shear resistance in the baked binder. Therefore, QI is important for the mechanical strength of the baked CTP-based paste. The fact that SPL contains much less QI (0.9 wt.%, see **Table 1**

Table 1) may suggest that the baked paste could exhibit lower mechanical strength. Therefore, it is important to verify the effect of QI the mechanical strength of the baked electrode.

1.1.2. Thermophysical properties

Thermogravimetric analysis was performed on a pilot-scale instrument to evaluate the thermal stability of the binder samples via monitoring the mass loss at different temperatures. 120 g samples were heated between room temperature and 700 °C (heating rate is 20 °C/h) under N₂ flow of 100 L/h to avoid oxidation. One of the main advantages of coal tar pitch binders is their high thermal stability, remaining practically unchanged up to >300 °C due to its aromatic nature (see **Figure 3**). The derivative thermogravimetric (DTG) curve exhibits a maximum mass loss rate at approximately 450 °C, corresponding to the carbonization stage and greatest volatile release.

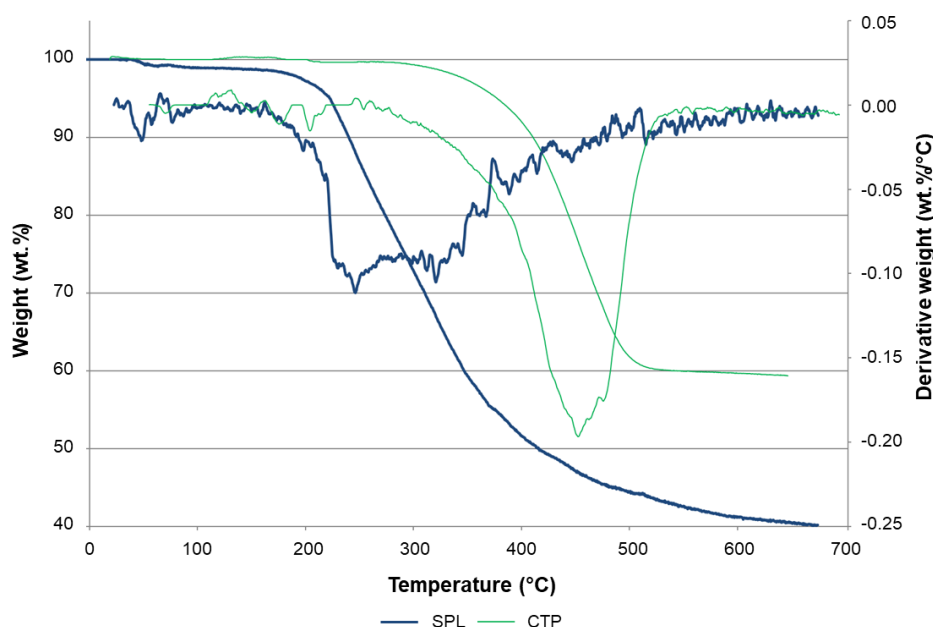


Figure 3. Thermogravimetric analysis of binder samples.

In contrast, solid pyrolytic lignin begins to degrade at temperatures as low as 50 °C, with a moderate release of volatiles up to around 200 °C, after which significant carbonization occurs. DTG shows a broad negative peak near 250 °C-300 °C, indicating the main decomposition event (the polymerization reactions) takes place around that temperature region, and spread over a wide range of temperatures (multi-step reactions, compared to CTP. SPL's devolatilization in a narrower temperature band during baking (once it accelerates) can produce gas evolution faster than it can diffuse out, causing internal pressure, swelling, and foam-like char morphologies, as in **Figure 4**. This pronounced difference in thermal stability presents challenges in preparing aggregate-binder mixtures, as the narrow safe operational window requires precise temperature control to avoid undesired volatile release and viscosity changes in the mixture.



Figure 4. Foam-like SPL char, formed during TGA test.

The absolute density of the binder samples was measured by helium pycnometer at 25 °C according to ISO 1183-1A. Solid pyrolytic lignin exhibited a slightly lower absolute density than coal tar pitch (see **Table 2**), which is attributed to differences in the origin and composition of the two binder materials. The high density of CTP is related to its condensed, more aromatic structure, compared to SPL. However, in order to produce more robust electrodes, higher values of density would be required.

Table 2. Thermophysical properties of binder samples.

Parameter	SPL	CTP
Helium density, g/cm ³	1.1227	1.3017
Softening point (SP), °C	110.0	91.7

The rheological properties of the binder samples were measured with a rotational rheometer. Dynamic viscosity is a measure of binder fluidity during paste mixing stage. Solid pitch binder samples were pre-melted prior to analysis. For comparison, viscosity values were evaluated at temperatures between 150 and 180 °C (see **Figure 5**), since pyrolytic lignin showed greater thermal stability at this temperature according to thermogravimetric analysis. Viscosity of CTP showed monotonic decrease with increasing temperature, reaching a minimum of 0.13 Pa·s at 180 °C. Viscosity measurements suggest a broad mixing temperature window (170–180 °C is ideal range).

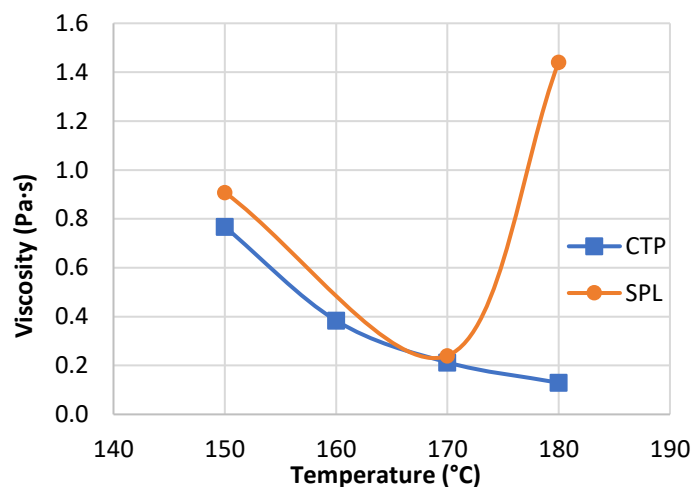


Figure 5. Viscosity of SPL and CTP at different temperatures.

Viscosity of SPL followed the same trend as CTP, with a pronounced decrease between 150 °C and 170 °C. However, higher temperatures resulted in a sudden increase in viscosity, as the viscosity at 180 °C (1.4 Pa·s), which is significantly higher than that at 150 °C (0.91 Pa·s), as in **Figure 5**. This is consistent with onset of condensation and crosslinking reactions that raise molecular weight and form a gel-like network, increasing viscosity at temperatures higher than 170 °C. This characteristic behavior reflects thermal instability of SPL. Based on the viscosity measurements, the mixing temperature window of the SPL-based paste is narrow and should not exceed 170 °C to avoid premature polymerization and ensure proper binder flow and wetting.

The softening point of binder samples is the temperature at which it transforms from a solid state to a liquid state and was measured by Mettler standard method (ASTM D3104-99 (2010)). Solid pitch binder samples were pre-melted at 50 °C above their estimated softening point and molded before analysis. Coal tar pitch is the preferred electrode binder owing to its adjustable softening point and unique thermophysical properties. For comparison, a benchmark coal tar pitch binder with a softening point of 90 °C was selected. The mixing temperature depends on the softening point of the binder. It should be high enough to reduce the binder viscosity and improve the interaction between the dry aggregates and the liquid binder. The high softening point of SPL (110 °C) means that the mixing temperature of the bio binder-based paste might be higher than that of CTP-based paste to obtain good paste consistency.

In summary, the thermophysical properties of bio- and fossil-derived binders were compared. To meet carbon electrode specifications, pyrolytic lignin should exhibit higher thermal stability, absolute density and more consistent thermo-viscous behavior, along with a lower softening point. An increase in absolute density can be achieved by incorporating densifying fillers, such as carbon black, which also enhance the coking value and carbonization yield of the bio-binder, as will be discussed in the following section. Nevertheless, the addition of such fillers can

significantly raise the binder's softening point and viscosity, thereby complicating its mixing with the aggregate, as a higher temperature would be required to ensure proper blending. A study on the effect of incorporating carbon black at low concentrations (5–10 wt%) on the chemical composition and thermophysical properties of pyrolytic lignin is provided in **Table 3**.

Table 3. Chemical composition in wt% and thermophysical properties of binder samples with carbon black (CB) addition.

Sample	C (%)	H (%)	N (%)	S (%)	O (%)	QI (%)	ρ (g/cm ³)	SP (°C)
SPL	70.6	7.2	0.1	0.01	21.9	0.0	1.1227	110.0
SPL/CB (95/5)	71.9	6.9	0.1	0.01	21.0	5.6	1.2176	121.8
SPL/CB (90/10)	73.1	6.4	0.1	0.01	20.4	9.0	1.2689	122.8

QI: Quinoline Insoluble; **ρ :** Absolute density; **SP:** Softening Point

Carbon black was homogeneously dispersed in the binder matrix by heating the binder to 150 °C, adding the carbon black, and stirring the mixture for 30 min. As the carbon black concentration increases, the carbon content in the binder also rises, since carbon black is primarily composed of elemental carbon, and, consequently, the concentration of other major elements, such as oxygen and hydrogen, decreases. Although SPL initially shows a negligible concentration of quinoline insolubles, this value increases significantly upon addition of carbon black. This is consistent with the literature, as carbon black acts as nuclei for the growth of QI particles in the binder matrix [24]. Moreover, using carbon black as a densifying agent has the expected effect on helium density, increasing it as the concentration rises. However, the drawback is that the softening point increases by more than 10 °C, which translates into a higher energy input required in the subsequent blending with the aggregate.

1.1.3. Wettability

Ensuring good wettability of the binder on an aggregate is essential during the mixing step in carbon electrode paste manufacture [25]. The interaction between the binder and the substrate depends on several factors: (i) the thermophysical properties of the binder (e.g., softening point, surface tension, viscosity), (ii) the morphology of the aggregate (e.g., particle size, texture, porosity), and (iii) chemical interactions, including hydrogen bonding, π - π interactions from C=C bonds, condensation reactions, and acid–base or other electrostatic interactions arising from differences in polarity and surface chemistry [26].

The wettability of binder samples on flat particles of reference aggregates commonly used in electrode pastes—calcined petroleum coke (CPC) and electrically calcined anthracite (ECA)—was investigated using the sessile drop technique in a horizontal observation furnace with a motorized carriage. Tests were conducted at 178 °C, corresponding to the typical mixing temperature in commercial paste production, under an inert argon atmosphere. The contact angle, which measures the pitch’s ability to spread over the aggregate surface, was monitored over time, with smaller angles indicating better wettability [27].

In the case of electrically calcined anthracite, slow wetting of solid pyrolytic lignin is observed until the wetting point is attained (contact angle = 90°), after approximately 13 min (see **Figure 6**). Subsequently, more rapid wetting occurs. After around 30 min, the contact angle tends to stabilize at ~26°, indicating that the binder is well spread on the surface of the aggregate.

In general, binders with good wetting properties attain low contact angle values in a short time, as observed in the case of coal tar pitch, where a contact angle of ~16.5° is observed within 10 min. It is important to note that electrically calcined anthracite is non-porous, so binder wetting occurs only on the outer surface of the flat aggregate particles.

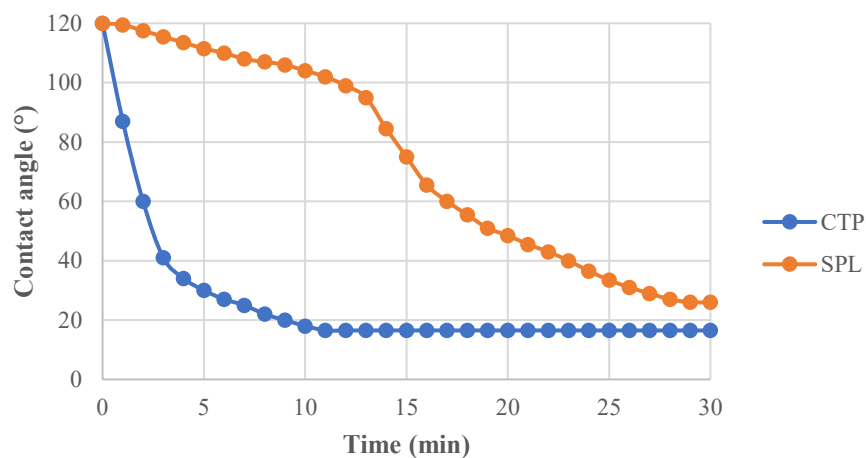


Figure 6. Study of wettability of binder samples on ECA at 178 °C.

In contrast, for calcined petroleum coke (see **Figure 7**), complete penetration (contact angle = 0°) of both binders is achieved within a short time (CTP: 8 min vs. SPL: 11 min), owing to the high porosity of petcoke.

2026-201629-0001 2026-02-04

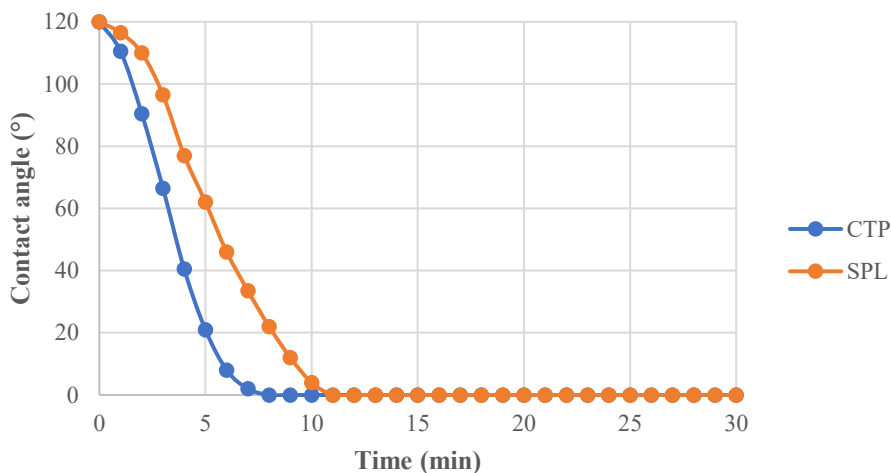


Figure 7. Study of wettability of binder samples on CPC at 178 °C.

Improving the wettability of solid pyrolytic lignin may require further modification of the bio-based binder’s chemical composition. Project partner BTG Biomass Technology Group provided a pyrolytic lignin sample that was post-processed via acetylation. This modification aimed at enhancing compatibility with reference aggregate samples by reducing the number of hydroxyl functional groups in the pristine binder.

Wettability studies of the acetylated SPL (Ac-SPL) on ECA and CPC aggregates indicated that reducing –OH groups (FT-IR: 3100–3600 cm⁻¹, see FTIR spectra in **Figure 8**) slightly improved the binder’s wettability due to changes in polarity, particularly on ECA, although it still did not reach the level observed for CTP. Since these aggregates are primarily apolar owing to their fossil carbon origin, the more apolar acetylated SPL exhibited better affinity toward them.

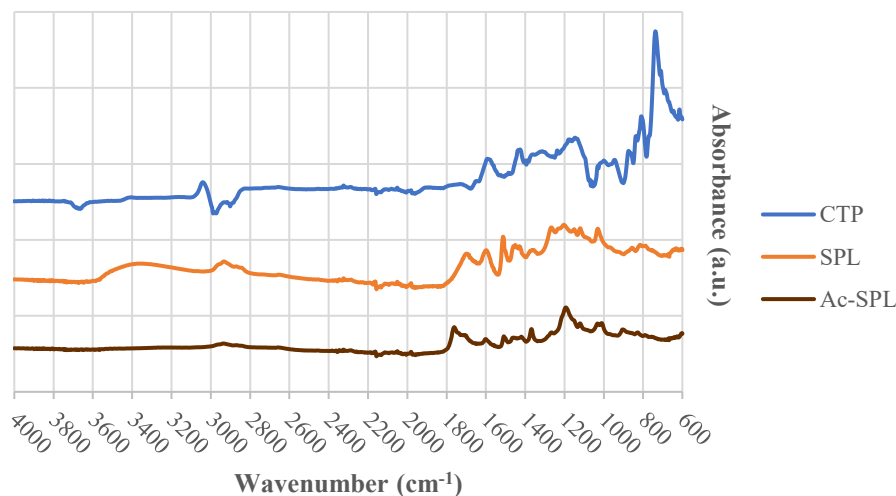


Figure 8. FT-IR spectra of binder samples, including Ac-SPL.

2026-02-04

2026-201629-0001

A significant difference in the wettability of anthracite is observed when comparing unmodified and post-processed pyrolytic lignin under the same temperature conditions (see **Figure 9**). The wetting point (contact angle = 90°) is reached after 6 min for the acetylated sample, compared to 13 min for the unmodified sample. Furthermore, the contact angle of the acetylated sample stabilizes approximately 4 min earlier than that of its unmodified counterpart (25 vs. 29 min).

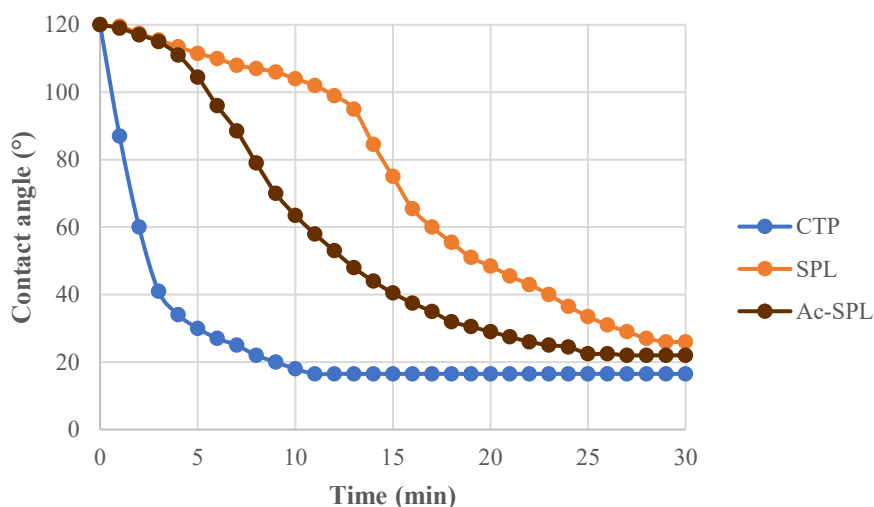


Figure 9. Study of wettability of binder samples on ECA at 178 °C, including Ac-SPL.

In turn, the wettability of the acetylated sample on petroleum coke shows only a slight improvement compared to the unmodified sample (see **Figure 10**). Both the wetting point and complete penetration are reached at similar contact times for both pyrolytic lignin binders.

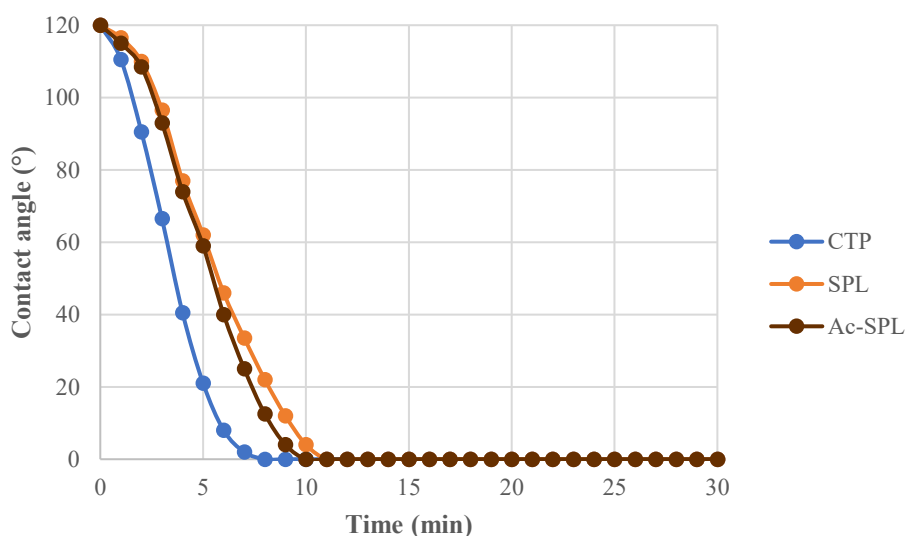


Figure 10. Study of wettability of binder samples on CPC at 178 °C, including Ac-SPL.

1.2. Characterization techniques after carbonization

1.2.1. Carbonization performance

The coking value is a parameter that indicates the amount of carbonaceous residue remaining after the pyrolysis of pitch. It is typically determined using standard test method ISO 6998:1997 in which the pitch is calcined at 550 °C in an electric furnace for 150 minutes in an inert atmosphere. High coking value binder is desired as less volatiles are removed from the paste in the baking step, resulting in baked electrode with minimum porosity, cracks and air permeability. When comparing the coking values of bio-based and fossil-derived binders, a significant difference is observed (**Table 4**). The high coking value of CTP is attributed to its aromatic nature. SPL, in contrast, contains high concentrations of aliphatic and O-containing chemical compounds. These components are less stable than the aromatic compounds at elevated temperatures, and consequently solid pyrolytic lignin has low coking value. In order to meet pitch specifications, SPL should exhibit a coking value of at least 55–60 wt%.

Table 4. Carbonization performance of binder samples.

Parameter	C-SPL	C-CTP
Coking value, wt%	44.1	68.9
Carbonization yield, wt%	36.6	57.4

The binder samples were carbonized at 1100 °C in closed alumina crucibles. These crucibles were placed inside larger ones and covered with coke particles before being heated in a muffle furnace. As expected, due to the significant differences in thermal stability and coking value between the binder samples, the carbonized pyrolytic lignin exhibited a considerably lower yield than the carbonized coal tar pitch.

Several strategies have been proposed to enhance both the coking value and the carbonization yield, such as blending solid pyrolytic lignin with carbon black (CB) in concentrations of 5–10 wt%. **Table 5** shows that increasing the carbon black concentration results in a higher coking value. However, the coking value of 55–60 wt% required to meet pitch specifications was not achieved. Moreover, a higher carbon black addition would negatively affect the thermophysical properties of the pitch, as observed in **Table 3**.

Table 5. Carbonization performance of binder samples with carbon black (CB) addition.

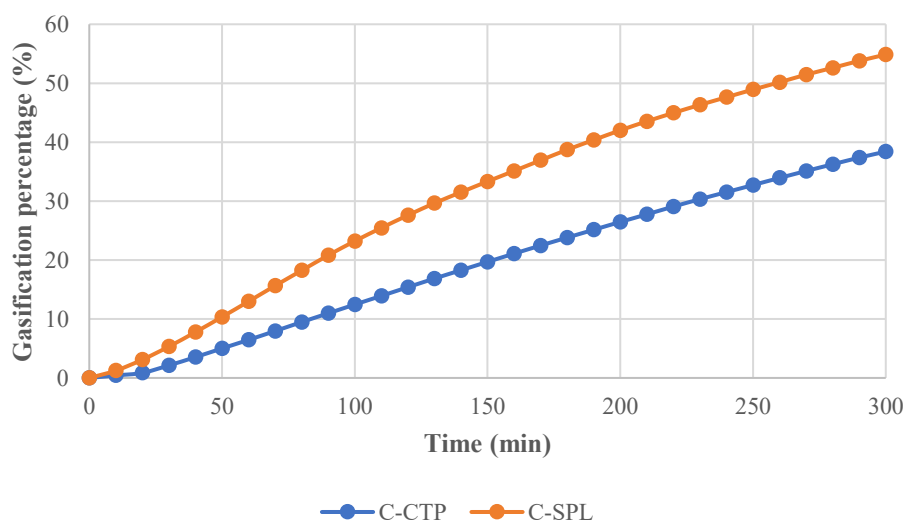
Sample	Coking value (wt%)	Carbonization yield (wt%)
SPL	44.1	36.6
SPL/CB (95/5)	48.2	40.5
SPL/CB (90/10)	51.4	43.3

1.2.2. Air and CO₂ reactivity

The air and CO₂ reactivity of the carbonized binders was studied by thermogravimetric analysis. The target temperature for the reactivity tests was reached under inert conditions before the reactive gas (air or CO₂) was introduced.

Air reactivity was investigated at 525 °C (**Figure 11**

Figure 11). Oxidation (air burn) occurs through the reaction between the exposed upper surface of the electrode and atmospheric oxygen [28]. Under these conditions, carbonized pyrolytic lignin appears to be approximately 50 % more reactive than carbonized coal tar pitch, which can be attributed to its less ordered carbon structure.


Figure 11. Air reactivity of carbonized binder samples at 525 °C.

CO₂ reactivity was investigated at 960 °C (**Figure 12**). The Boudouard reaction occurs when electrochemically generated CO₂ reacts with the carbon anode to form CO [29]. Interestingly, the CO₂ reactivity of carbonized pyrolytic lignin is less than half that of carbonized coal tar pitch. This value should be compared with the corresponding value for the carbon electrode prototype to verify the enhanced CO₂ resistance.

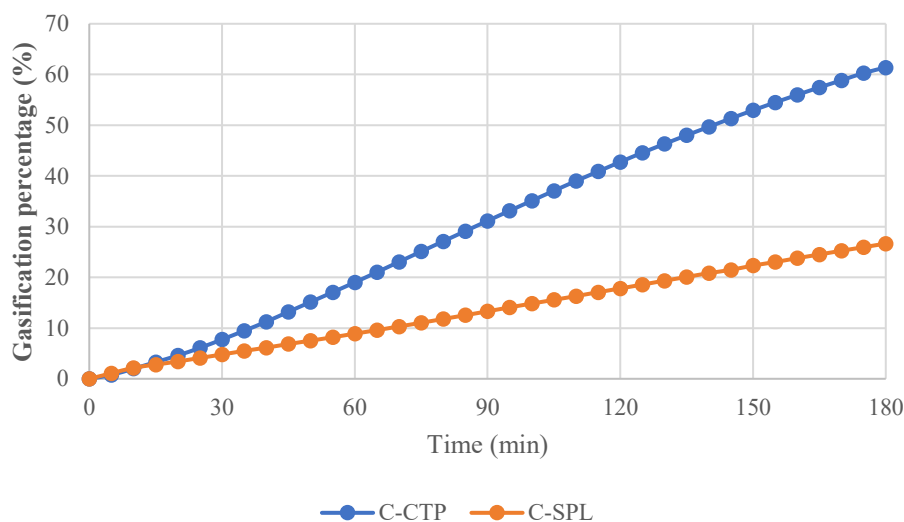


Figure 12. CO₂ reactivity of carbonized binder samples at 960 °C.

1.2.3. Graphitizability

Graphitizability is a crucial property of carbon materials used in electrode applications. Coal tar pitch binder is readily graphitizable and, due to its excellent electrical, mechanical, and thermal properties, is widely employed in electrode manufacturing [30].

Graphitization involves the transformation of disordered carbon into a polycrystalline graphite structure, a process that is thermodynamically exothermic but kinetically slow, requiring thermal treatment up to 3000 °C for completion [31]. This disordered structure, known as turbostratic carbon, is characterized by graphene layers stacked roughly parallel and equidistant but with random rotational orientation, resulting in misaligned basal planes.

Accordingly, carbon materials can be classified into (a) graphitizing carbon, in which neighboring crystallites tend to align nearly parallel, facilitating crystallite growth, and (b) non-graphitizing carbon, in which random orientation and extensive cross-linking hinder growth, producing isotropic structures with fine porosity [32].

To evaluate the graphitizability of carbon materials, characterization techniques such as X-ray diffraction (XRD) and Raman spectroscopy were employed. X-ray diffraction was employed to determine the crystallinity and degree of graphitization of the carbonized binders. The average crystallite size along the c-axis (L_c) was calculated using the Scherrer equation (1) [33], whereas the degree of graphitization (g) was quantified using the Méring–Maire equation (2) [34].

$$\text{Scherrer equation: } L_c(\text{\AA}) = \frac{0.89 \cdot \lambda}{\beta \cdot \cos \theta} \quad (1)$$

In this equation:

- λ : X-ray wavelength (1.5406 Å for Cu K α)
- β : full width at half maximum (FWHM) of the diffraction peak in radians
- θ : Bragg angle of the peak in radians

$$\text{Mering-Maire equation: } g (\%) = \frac{0.3440 - d_{002}}{0.3440 - 0.3353} \cdot 100 \quad (2)$$

In this equation:

- 0.3440 nm represents the lowest possible value of interplanar spacing (d_{002}) in a turbostratic carbon.
- 0.3354 nm (or 335.4pm) represents the interplanar spacing (d_{002}) of graphite.

Table 6. Graphitization characteristics of binder samples.

Parameter	C-SPL	C-CTP
Crystallite size (L_c), Å	12.0	25.1
I_D/I_G ratio	2.04	1.52

Carbonized pyrolytic lignin exhibits a relatively low crystallite size compared to carbonized coal tar pitch (see **Table 6**). However, neither of the carbonized binders can be classified as turbostratic carbon, as their diffraction patterns deviate significantly from that of graphite (26.5°) (see **Figure 13**). This deviation results in a calculated degree of graphitization below zero, indicating that the carbon structure is highly disordered and far from the ideal graphite lattice [32].

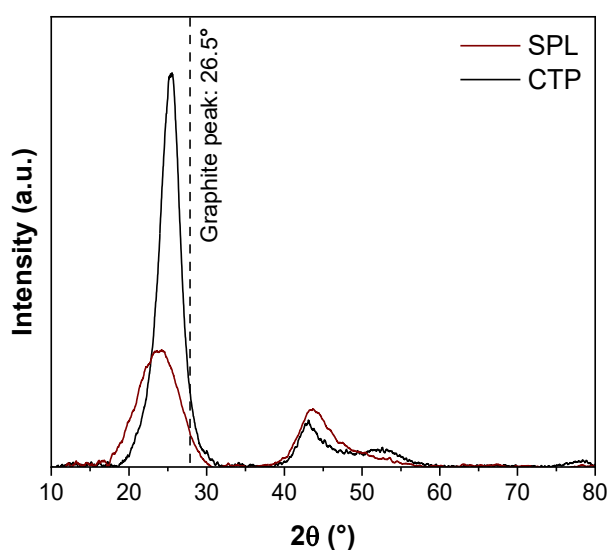


Figure 13. XRD patterns of binder samples.

Raman spectroscopy was employed to compare their relative amounts of amorphous and graphitic carbon. The degree of disorder in the carbonized materials was estimated by the ratio of the integrated values of the D-band and G-(graphitic) bands (I_D/I_G). The G-band is a resonant band observed in both graphene and graphite at $\sim 1580\text{ cm}^{-1}$, representing the planar configuration of symmetrically sp^2 -bonded carbon in graphene, while the D-band is a resonant band found at $\sim 1350\text{ cm}^{-1}$, indicating defects and disordered in the carbon material (see **Figure 14**) [35]. In line with the XRD results, carbonized solid pyrolytic lignin shows a higher degree of disorder than carbonized coal tar pitch, owing to its hard carbon nature (see **Table 6**).

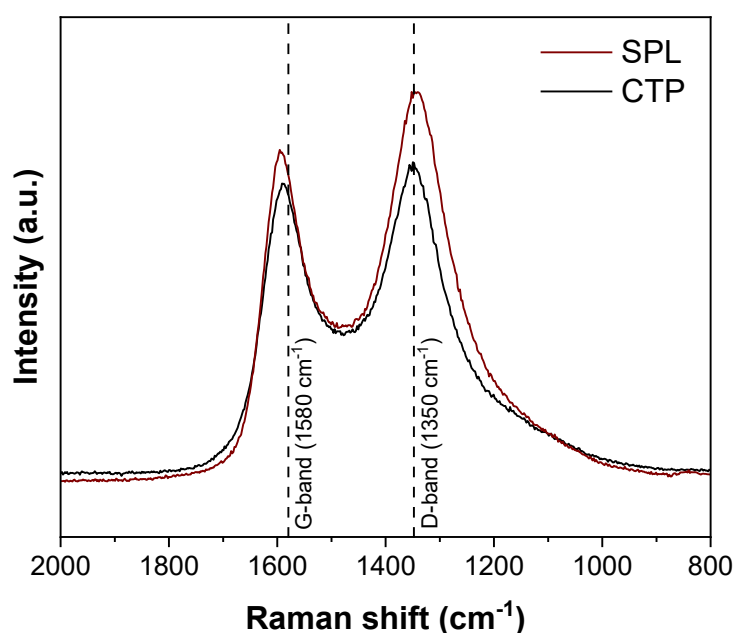


Figure 14. Raman spectra of binder samples.

1.3. Summary and conclusions of Work Package 1

The material characterization carried out in this work package provided a comprehensive comparison of fossil-derived and bio-based binders to assess the feasibility of using pyrolytic lignin (SPL) derived from Swedish biomass feedstocks as a sustainable alternative for carbon electrode production. The results highlight significant differences in their thermophysical properties, rheological behavior, wettability, carbonization performance, and graphitizability.

Coal tar pitch (CTP) exhibits higher absolute density, thermal stability, and coking value, which can be attributed to its more condensed and aromatic structure. These characteristics make it a binder well suited to meet Söderberg electrode specifications. In contrast, SPL shows lower thermal stability, a narrower processing window, and a lower coking value due to its high content of aliphatic

and oxygen-containing compounds, which are less stable at elevated temperatures. Consequently, the carbonized yield of SPL is lower than that of CTP.

Reactivity tests showed that carbonized SPL is more reactive to air than carbonized CTP, reflecting its highly disordered carbon structure. Interestingly, its reactivity to CO₂ is considerably lower, suggesting different driving factors and highlighting the need for verification at larger scales. XRD and Raman analyses confirmed that SPL-derived carbon is more disordered and less graphitized than CTP-derived carbon due to its hard-carbon nature. Unlike the soft-carbon CTP, SPL may require the addition of a catalyst to achieve a more ordered and graphitic structure.

Modification strategies, such as acetylation of SPL or blending with carbon black, can enhance key properties, including wettability, absolute density, coking value, and carbonization yield. However, the addition of carbon black may also increase the quinoline-insoluble content, softening point, and viscosity, which can complicate processing and mixing with aggregates.

Overall, while bio-based SPL presents a sustainable alternative to fossil-derived binders, further optimization of the thermochemical fractionation process to improve its composition, thermal stability and other key properties is needed to enhance performance and meet the requirements of carbon electrode applications.

2. Work package 2: Graphitization of solid pyrolytic lignin

Catalytic graphitization is a promising approach for transforming hard carbon materials, such as lignocellulosic biomass derivatives, into highly graphitic structures. Numerous catalysts have been shown to significantly accelerate the graphitization of both soft and hard carbons [36]. In the literature, graphitization catalysts are generally classified into three main categories: i) transition metals in their elemental, oxide, salt, or alloy forms; ii) boron and its derivatives; and iii) structured carbon-based materials, such as graphene oxide.

A typical catalytic graphitization process involves several stages: pre-treatment, optional pre-carbonization, catalyst incorporation, graphitization, and, in some cases, catalyst removal [37]. While transition metals and boron-based catalysts often require removal to achieve the high purity levels demanded for specific applications, structured carbon-based catalysts offer the advantage of not needing separation due to their compositional similarity with graphite [38].

The degree of graphitization depends on several factors, including the choice of carbon precursor, catalyst type and loading, heat treatment temperature, and the use of activating agents or pre-treatments. Higher catalyst loadings and elevated temperatures generally promote the growth of larger crystallites and more ordered carbon structures, facilitating the formation of graphitic nanostructures that eventually evolve into graphite [14].

A study of graphitizability was carried out using fine reduced iron powder as a catalyst [39], considering temperature and catalyst concentration in the mixture as variables. Elemental iron in powder form has been chosen as catalyst because previous studies on the catalytic graphitization of biomass-derived hard carbons have shown that this form exhibits higher degrees of graphitization than those achieved either in physical mixtures with iron oxides or as iron salts pre-adsorbed onto the raw biomass [40]. Furthermore, it has also been observed in literature that the use of metals in the form of fine powders favours graphite formation [14].

Other catalysts, such as boron oxide, boric acid, and graphene oxide, have also been evaluated for the graphitization of pyrolytic lignin. Boron-based catalysts present limitations due to their challenging separation from the carbon matrix of baked electrodes and the potential introduction of boron impurities into metallic products. In contrast, graphene oxide is a promising graphitization catalyst, as its compositional similarity to graphite allows direct incorporation into the electrode without requiring post-treatment removal

2.1. Synthesis of Fe-graphitized pyrolytic lignin samples

To achieve a homogeneous dispersion of the catalyst in the bio-based binder, the pyrolytic lignin is first melted before catalyst addition. The solid binder is placed in a beaker within a silicone oil bath and heated to 150 °C. This temperature was chosen because thermal stability tests showed minimal mass loss and suitable

viscosity at this point. Once the desired viscosity is reached, the catalyst powder is added and mixed with a rotary mixer for one hour. Different concentrations of fine iron powder ($<10\ \mu\text{m}$), ranging from 2.5 to 10 wt%, were tested. Higher concentrations were not considered, as the presence of iron can alter the thermophysical properties of the binder and act as an unintended catalyst, accelerating electrode consumption by air and CO_2 [10].

Once the binder has solidified, it is crushed and placed in an alumina crucible. The crucible is then covered by a larger outer crucible and surrounded with coke particles to create a local inert atmosphere around the sample. The binder samples are carbonized in a muffle furnace at temperatures ranging from 1100 to 1300 °C, limited by the furnace's maximum temperature. After graphitization, the samples are removed from the crucibles, washed with concentrated HCl for 2 hours at room temperature, filtered, and dried to remove any remaining catalyst.

To achieve full graphitization of pyrolytic lignin, the most promising Fe-containing binder was sent to Elkem Carbon Solutions facilities and graphitized at 2000 °C in their graphitization furnace. Beforehand, the sample was pre-carbonized at 1000 °C to stabilize the binder material. As the initial acid leaching was not fully successful, the same HCl solution was used, but the leaching temperature was increased to 80 °C to improve efficiency [41].

2.2. Characterization of Fe-graphitized pyrolytic lignin samples

X-ray diffraction was used to determine the crystallinity of the Fe-graphitized binder samples. A graphite monochromator was used to improve the quality of the XRD patterns by reducing background and fluorescence from Fe-containing phases. The crystallite sizes of the Fe-graphitized binder samples were compared at different Fe powder concentrations and graphitization temperatures. Pyrolytic lignin and coal tar pitch samples carbonized at 1100 °C were used as reference non-graphitizing and graphitizing carbons, respectively.

Fe-graphitized samples at 1100 °C show higher crystallite size (L_c) values than their counterparts carbonized at the same temperature in the absence of a catalyst, regardless of their carbon nature, thereby confirming the catalytic activity of the iron powder even at low temperatures. In general, the crystallite size increases with both catalyst concentration and graphitization temperature (see **Figure 15**). It has been observed that at the lowest catalyst concentration, the crystallite size remains relatively constant ($\sim 47\ \text{\AA}$) regardless of temperature. In contrast, at higher catalyst concentrations, the crystallite size increases proportionally with graphitization temperature, reaching a maximum value (104.3 Å) at 10 wt% Fe and 1300 °C. By examining the crystallite size within the temperature range of 1100–1300 °C, it is observed that catalyst concentration has a greater effect than graphitization temperature, as samples with certain catalyst concentrations at maximum temperatures do not reach the minimum values of samples with higher catalyst

2026-201629-0001 2026-02-04

concentrations. However, the crystallite size increases significantly when the graphitization temperature is raised to 2000 °C, reaching a value of 275.0 Å.

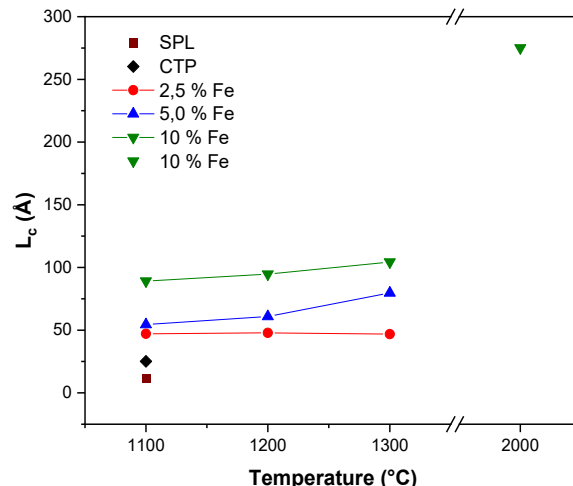


Figure 15. Crystallite size (L_c) of Fe-graphitized binder samples.

The Fe-graphitized binder samples containing 10 wt% Fe at 1300 and 2000 °C serve as examples for comparing the XRD patterns of both carbonized (C-SPL) and Fe-graphitized Solid Pyrolytic Lignin (Fe-G-SPL) (see Figure 16). In contrast to the carbonized binder sample, which exhibits a broad peak centered around $\sim 23.5^\circ$, the Fe-containing binder sample graphitized at 1300 °C displays a sharp peak at 26.24° , which is very close to that of pure graphite (26.5°), confirming its graphitic nature. The degree of graphitization (g) for this particular sample is 54%. The other sharp but less intense peaks observed correspond to Fe_xO_y , as Fe was only partially removed by acid leaching with HCl [42]. Conversely, the sample graphitized at 2000 °C shows a sharper and more defined peak, with a degree of graphitization of 94%. Several Fe_2O_3 patterns have diminished due to the more effective acid leaching.

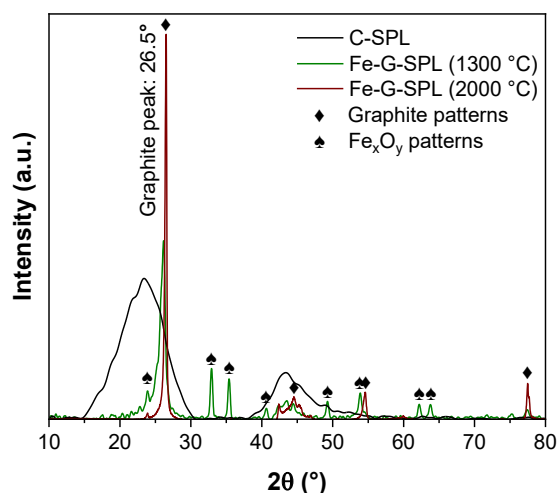


Figure 16. XRD patterns of graphitized binder samples with 10 wt% Fe at 1300 and 2000 °C.

To support the XRD results, Raman spectroscopy was employed to compare the relative amounts of amorphous and graphitic carbon in the Fe-graphitized binder samples. As discussed previously, the I_D/I_G ratio serves as a measure of the degree of disorder in the samples: the lower the I_D/I_G ratio, the higher the amount of graphitic carbon. As in the previous study, reference pyrolytic lignin and coal tar pitch carbonized at 1100 °C were included.

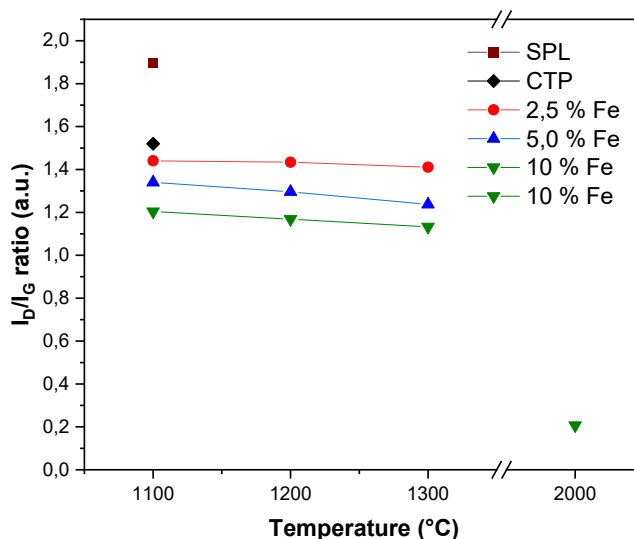


Figure 17. I_D/I_G ratio of Fe-graphitized samples.

As shown in **Figure 15**, when comparing I_D/I_G ratios of carbonized and Fe-graphitized samples at 1100 °C, those with the catalyst addition show higher values, regardless of their carbon nature (see **Figure 17**). A trend similar to that observed in crystallite size was noted for the I_D/I_G ratio of binder samples with 2.5 wt% Fe. The I_D/I_G ratio remained relatively constant (~ 1.43) as the graphitization temperature increased from 1100 to 1300 °C. In contrast, for higher catalyst concentrations, the I_D/I_G ratio decreased proportionally with graphitization temperature. Binder samples with 10 wt% Fe exhibited the lowest I_D/I_G values among all sets of experiments, reaching a minimum of 1.13 at 1300 °C, which is consistent with the XRD results. Raising the graphitization temperature to 2000 °C results in a significant difference in the degree of disorder, with the pertinent sample showing an I_D/I_G ratio of 0.21.

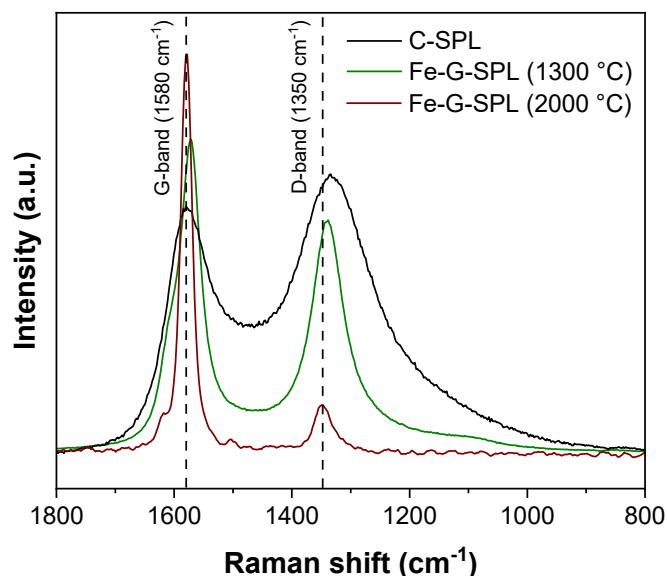


Figure 18. Raman spectra of graphitized binder samples with 10 wt% Fe at 1300 and 2000 °C.

The Fe-graphitized binder sample containing 10 wt% Fe at 1300 and 2000 °C also serve as examples for comparing the D- and G- bands of both carbonized (C-SPL) and Fe-graphitized. Solid Pyrolytic Lignin (Fe-G-SPL) (see **Figure 18**). In contrast to the carbonized binder sample, which exhibits a broader and more intense D-band than its G-band, the Fe-graphitized binder samples display narrower D-bands and a more intense G-bands. These results are consistent with the graphitization degrees obtained from XRD for the Fe-graphitized binder samples, indicating that they are partially ($g = 54\%$ at 1300 °C) and nearly fully graphitic ($g = 94\%$ at 2000 °C).

The surface morphology of Fe-graphitized binder samples was examined by Scanning Electron Microscopy (SEM). **Figure 19a** shows the morphology of pyrolytic lignin carbonized at 1100 °C, exhibiting a highly amorphous structure characteristic of disordered hard carbon. **Figure 19b** presents a benchmark graphite powder, displaying a well-defined layered morphology. The binder sample graphitized with 10 wt% Fe at 1300 °C (**Figure 19c**) remains largely amorphous, though slightly layered features appear at the edges. Energy-dispersive X-ray spectroscopy (EDS) analysis of this region (**Figure 19d**) confirmed the presence of iron particles. Acid leaching with HCl was only partially successful; however, the residual Fe particles are significantly smaller than those introduced during synthesis ($<10\ \mu\text{m}$). In contrast, the binder sample graphitized at 2000 °C (**Figure 19e**) exhibits a more ordered, plate-like morphology, closely resembling the benchmark graphite [43]. Nevertheless, even with the increased leaching temperature, a spherical iron particle ($<5\ \mu\text{m}$) remains visible in the graphitized sample (**Figure 19f**).

2026-201629-0001 2026-02-04

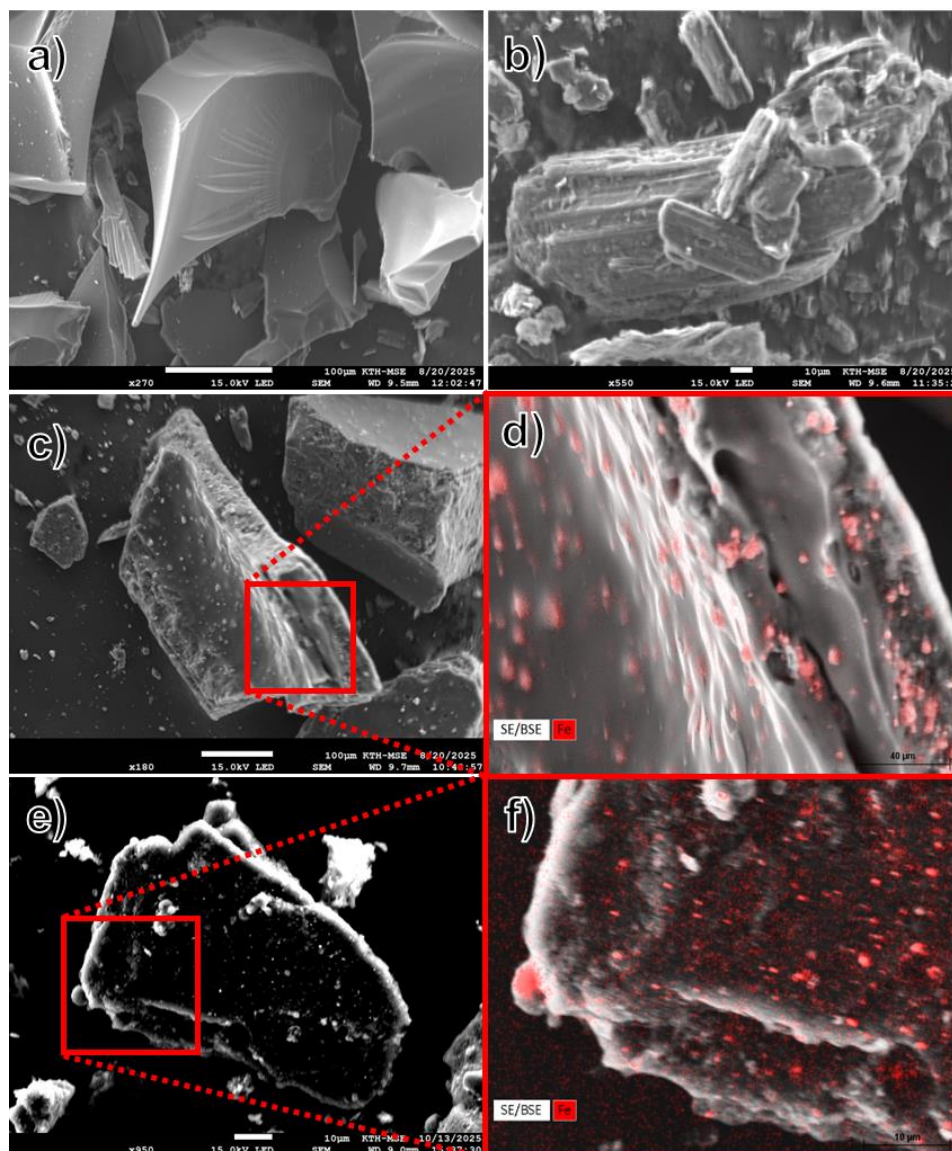


Figure 19. SEM-EDS micrographs: (a) Carbonized SPL; (b) Benchmark graphite powder; (c) Fe-graphitized binder sample with 10 wt% Fe at 1300 °C; (d) Magnification of Fe-G-SPL (1300 °C) with EDS analysis; (e) Fe-graphitized binder sample at 2000 °C (f) Magnification of Fe-G-SPL (2000 °C) with EDS analysis.

2.3. Synthesis and characterization of pyrolytic lignin graphitized with boron and graphene oxide

As briefly mentioned above, boron-based and structured carbon catalysts were also evaluated as alternative systems for the catalytic graphitization of a pyrolytic lignin binder. Below are described the synthesis routes pursued to obtain graphitic materials using commercial catalysts from both families:

Boron-containing compounds (B_2O_3 and H_3BO_3) were selected as graphitizing agents [44]. To ensure a consistent comparison, the compositions were adjusted to contain 6 wt.% boron oxide in each case. Boron precursors were first mechanically

mixed with pyrolytic lignin at room temperature using a pestle and mortar to obtain a uniform mixture. The mixtures were then placed in alumina crucibles, covered with alumina lids, and embedded in larger alumina crucibles filled with coke to maintain a reducing environment during carbonization-graphitization. Heat treatment was carried out as follows: (i) the samples were heated to 100 °C and held for 4 h; (ii) then raised to 500 °C and maintained for 1 h; (iii) subsequently increased to 1000 °C and kept for 5 h; and (iv) finally cooled to room temperature at an approximate rate of 16 °C/min.

As an alternative approach, solid pyrolytic lignin (SPL) was dispersed in a 4 mg/mL aqueous graphene oxide (GO) suspension and stirred at 70 °C for 3 h, forming a gelatinous slurry. Excess 2-propanol was added to prevent solvent evaporation while mixing [45]. The slurry was subsequently cured at 150 °C for 12 h. After curing, the material was ground and pyrolyzed at 1200 °C for 1 h in a muffle tube furnace under a continuous flow of argon at 100 mL/min. The weight ratio of GO/SPL was varied from 1:200 to 1:50 to investigate the effect of GO concentration on the resulting hard carbon materials [38].

Characterization results for both catalyst families are presented in **Figure 20** in terms of crystallite size and degree of disorder. For reference, L_C values and I_D/I_G ratios of coal tar pitch and pyrolytic lignin carbonized at 1100 °C are also shown. XRD results show that the crystallite size values of both boron- and graphene oxide-catalyzed samples are of the same order of magnitude as that of carbonized pyrolytic lignin, indicating that graphitization was ineffective. Although the crystallite size values for boron-catalyzed samples are practically the same due to the equivalent boron oxide concentration, samples with higher GO/SPL ratios exhibit a slightly increased crystallite size. This is attributed to the inherent graphitic structure of graphene oxide, which contributes to the crystallite size even at low concentrations.

Raman spectroscopy results are consistent with the XRD data, showing that the degree of disorder in samples from both catalyst families is comparable to that of carbonized pyrolytic lignin, supporting the conclusion that graphitization was limited. Notably, the I_D/I_G ratios of GO/SPL samples with ratios of 1:80 and 1:50 are approximately intermediate between those of carbonized coal tar pitch (CTP) and SPL.

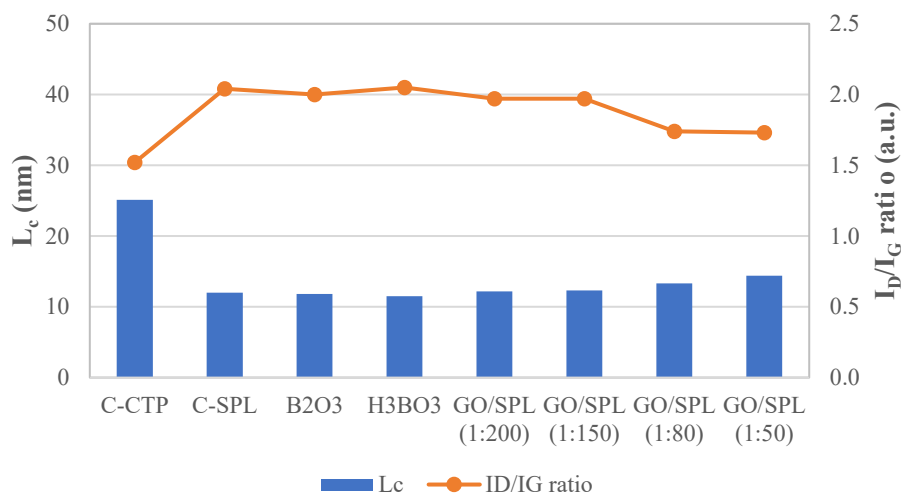


Figure 20. Crystallite size (L_c) and I_D/I_G ratio of graphitized samples with boron and GO.

To better understand these observations, the following explanations are proposed. In the case of boron-containing catalysts, the heating temperature may have been insufficient to induce graphitization of the materials. The temperatures used were chosen based on literature reports and were not varied due to the limited availability of high-temperature furnaces. The boron-catalyst route was not further pursued because its practical applicability in metallurgical processes is limited. Boron is not easily separable from carbon without damaging electrode integrity and must therefore be present at very low concentrations, as it can readily transfer to metallic products during metallurgical and steelmaking operations, leading to contamination and degradation of product quality. In addition, this constraint also significantly limits its catalytic activity.

Regarding graphene oxide-catalyzed graphitization, the limited success can be attributed to the compositional heterogeneity of pyrolytic lignin. Previous studies that inspired this work employed raw materials with more uniform structures, such as furan resins, which enable effective crosslinking between the functional sites of the resin and graphene oxide. Furthermore, differences in viscosity and softening point between furan resins and lignin hinder the uniform dispersion of graphene oxide and its effective crosslinking with the binder. Several dispersion methods, including ultrasonication followed by physical mixing, combined with adjustments to mixing and curing conditions (temperature and time), have so far yielded limited improvements, underscoring the need for further process optimization.

Nevertheless, the GO-catalyzed approach remains a promising candidate for future research, as the catalyst's compositional similarity to graphite eliminates the need for its removal after graphitization, unlike Fe-based catalysts. Therefore, to enhance the efficiency of graphene oxide-induced graphitization, pyrolytic lignin with a more homogeneous composition should be targeted during the thermochemical fractionation of lignocellulosic biomass.

2.4. Summary and conclusions on Work Package 2

Characterization techniques used to evaluate the graphitizability of the Fe-graphitized binder samples confirmed that, although full graphitization was not achieved within the temperature range of 1100–1300 °C, the addition of 10 % fine reduced Fe powder is sufficient to induce graphitization of the originally hard carbon material, namely solid pyrolytic lignin. For the specific application in carbon electrode pastes, this degree of graphitization may be sufficient ($g = 54 \%$; $L_c = 104.3 \text{ \AA}$; I_D/I_G ratio = 1.13, at 1300 °C). It has been proved that raising the temperature up to 2000 °C can induce nearly full graphitization of the binder ($g = 94 \%$; $L_c = 275.0 \text{ \AA}$; I_D/I_G ratio = 0.21); however, excessively high iron concentration is not desirable, as it may adversely affect the thermophysical properties of the binder and complicate the removal of the iron catalyst from the carbonized binder material. Consequently, as previously discussed, incomplete removal of iron could enhance its reactivity with air and CO₂, accelerating future electrode consumption.

In this context, the removal of iron presents a significant challenge, as acid leaching of electrode paste is not industrially feasible due to the large volumes of corrosive solutions required. Alternative methods such as chloridizing roasting may be considered for the efficient removal of iron from baked electrodes. However, for certain industrial applications, such as Söderberg self-baking electrodes used in SAFs for ferroalloy production, iron catalysts could be maintained at low concentrations without compromising product quality. Therefore, the incorporation of Fe-containing bio-binder blends in the preparation of bio-carbon electrode prototypes will be explored in future research.

Alternatively, the use of structured carbon-based materials as graphitization catalysts, such as graphene oxide, offers the advantage that further separation is unnecessary due to their compositional similarity to graphite. Although research carried out during the current project indicated that the heterogeneous composition of SPL hinders effective cross-linking between the functional sites of both the binder and the catalyst, optimizing the thermochemical fractionation of lignocellulosic biomass to achieve a more homogeneous composition of SPL may enable effective catalytic graphitization of the binder during Söderberg paste self-baking process. TCF process optimization includes adjusting the operating conditions of fast pyrolysis and thermochemical fractionation, as well as incorporating post-processing steps based on thermal treatment and chemical refinement.

3. Work package 3: Application of pyrolytic lignin in the manufacture of bio-based Söderberg electrode pastes and refractory bricks

3.1. Preparation of laboratory scale Söderberg electrode paste

A mixture of electrically calcined anthracite and calcined petroleum coke were used as dry aggregates. The anthracite and coke were crushed then classified into different size fractions, according to a standard Elkem Carbon Solutions recipe. CTP with a softening point 90 °C was used to produce the reference paste, while SPL was applied in the test recipe. The dry aggregates and binders were preheated in a heating cabinet at 170 °C. Under preheating conditions, SPL started to boil, producing vapors with strong smell, compared to more stable CTP liquid.

A 30 L paddle mixer at the Elkem Carbon R&I lab was used to produce electrode pastes. Preparing SPL-based paste was difficult due to the thermal instability of the binder. Normally, preheated dry aggregate is put in the mixing bowl first, and liquid binder is added slowly, through an opening on top of the mixer, while mixing. However, because of the rapid change in SPL viscosity, the regular mixing procedure could not be used. Instead, all the liquid binder was added once to the preheated dry aggregates, as shown in **Figure 21**.



Figure 21. Preheated dry aggregate and molten binder inside the mixing bowl.

A mixing time of 45 minutes was applied to prepare the reference and test recipes. It is worth mentioning that due to the expected rheology shift during SPL preheating, it was necessary to increase the binder content in the test recipe to 5 % more than was used for CTP in order to obtain similar paste consistency.

3.2. Characterization of Söderberg electrode pastes and prototype electrodes

3.2.1. Plasticity and flow under heat

Söderberg paste, when heated, should fill the entire cross section of the electrode casing. The ability of paste to flow is measured by its plasticity, which is the percentage of diameter increase of a cylinder of paste sample after a defined heat treatment (at 300 °C to simulate the temperature conditions in the paste melting zone inside an industrial electrode). Electrode paste with plasticity between 20-60 % is considered a good paste, based on the metallurgical process and temperature conditions in the actual electrode. Below this plasticity range, the paste is dry and cannot fill the electrode casing. If the paste is too fluid, it may give rise to segregation which may cause electrode breakage.

Table 7 shows plasticity measurement of the SPL-based paste at different temperatures. The paste has acceptable flowability at relatively low temperature (43 % at 200 °C, which is acceptable). Increasing the temperature to 250 °C, resulted in a fluid paste (plasticity of 81 %) which could trigger segregation and consequently electrode breakage. Heating the SPL-based paste to 300 °C (the normal testing temperature of CTP-based paste) resulted in complete melting, violent devolatilization and immediate carbonization of the binder phase, as in **Figure 22**.

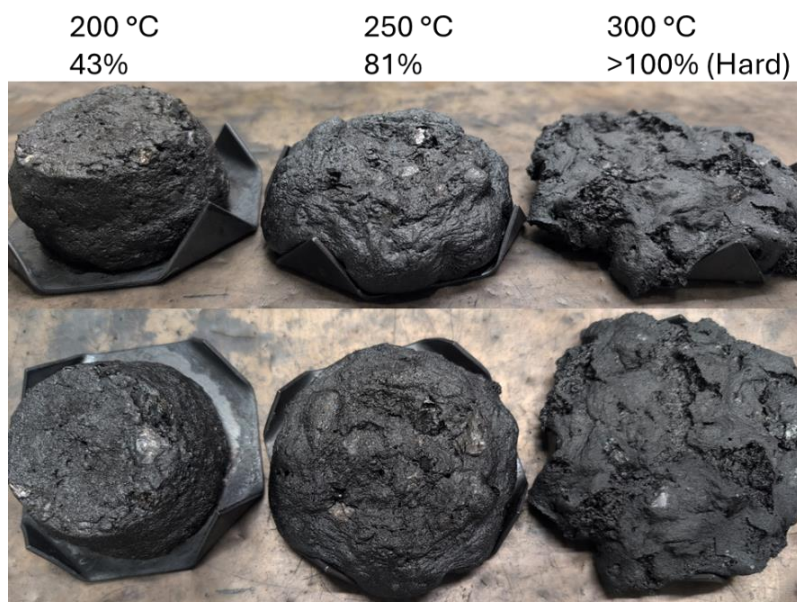


Figure 22. Plasticity samples of SPL-based paste at different temperatures.

Based on the observations during the plasticity test, SPL-based paste does not fit with the actual temperature profile inside the electrode column. Using the conventional slipping rate could trigger segregation within the electrode paste as well as early binder carbonization and paste solidification before complete filling

of the steel casing, causing defects and potential green electrode breakage. For that reason, SPL-based paste was baked at slower baking program, compared to the conventional CTP-based paste (the test electrode is slipped in the pit furnace at a 50 % slower rate).

Table 7. Plasticity (%) measurements at different temperatures.

Baking temperature (°C)	CTP-paste (%)	SPL-paste (%)
200	–	43
250	–	81
300	44	>100

3.2.2. Electrode paste baking

Fast heat treatment (500 °C, at ~100 °C/h)

To measure the coefficient of thermal expansion, 2 kg of the paste was loaded into a steel casing then baked at a maximum of 500 °C (100 °C/h in average). **Figure 23** shows the baked CTP-based sample. Due to the high thermal stability of CTP, the paste melts and then carbonizes inside the casing, with a relatively low rate of devolatilization. Therefore, the high heating rate used for that test did not result in any damage to the baked paste. The surface of baked paste was smooth and drilled core samples were free from large defects, as in **Figure 23c**.

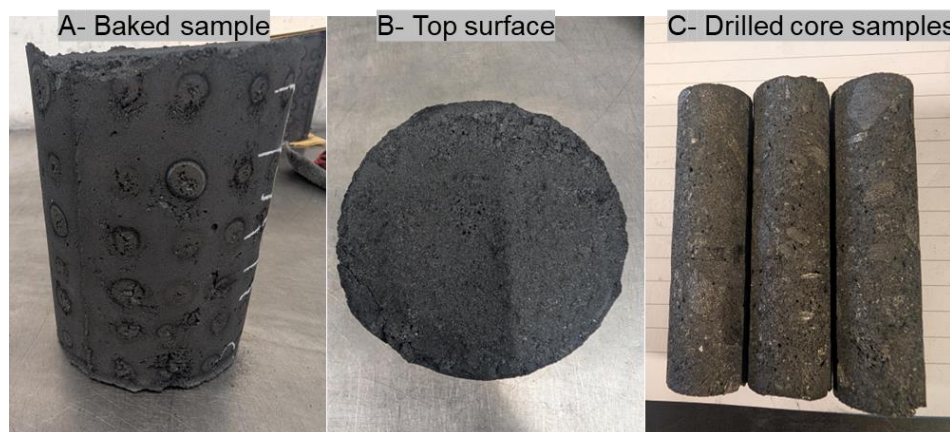


Figure 23. Baked CTP-based paste at 500 °C (100 °C/h).

Figure 24 shows the SPL-based sample, baked using the same heating program (500 °C at 100 °C/h). Fast heating rate used for the baking process resulted in rapid gas release, leading to significant expansion, pushing out the graphite lid. Violent devolatilization created a hole and cracks in the top of the baked sample and drilled cores were very porous, as shown in **Figure 24c**.

2026-201629-0001 2026-02-04

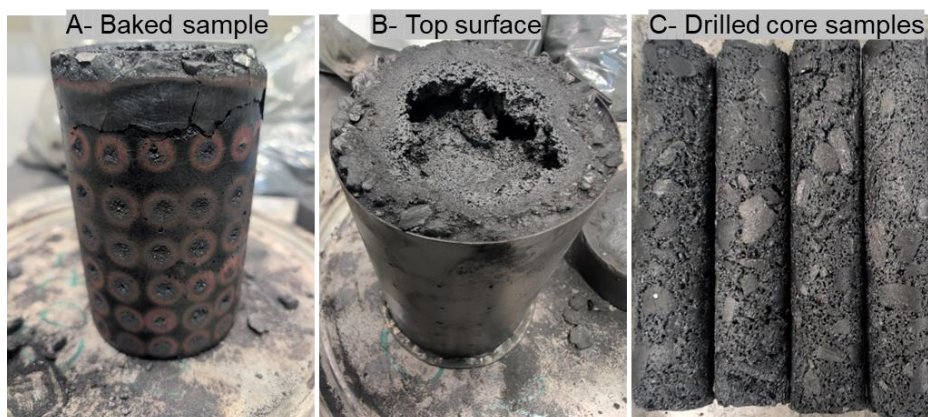


Figure 24. Baked SPL-based paste at 500 °C (100 °C/h).

Regular electrode baking regime

At Elkem Carbon Solutions R&I lab, the electrode paste is baked inside a steel casing using a program designed to mimic the baking of an electrode within an electrode column. Based on the above-mentioned observations, using the conventional heating rate to bake the SPL-based electrode paste could create porosity, induce cracks which negatively affect the final electrode properties. For that reason, SPL-based paste was baked at slower baking program.

Reducing the thermal ramp and increasing residence time in subcritical temperature zones allowed progressive devolatilization and densification, limiting pressure build-up and foaming. This also promotes better wetting and capillary redistribution before the onset of extensive crosslinking/carbonization. Consequently, baked electrode is visually similar to standard with drilled samples showing no pronounced cracks or excessive porosity, as in **Figure 25**.

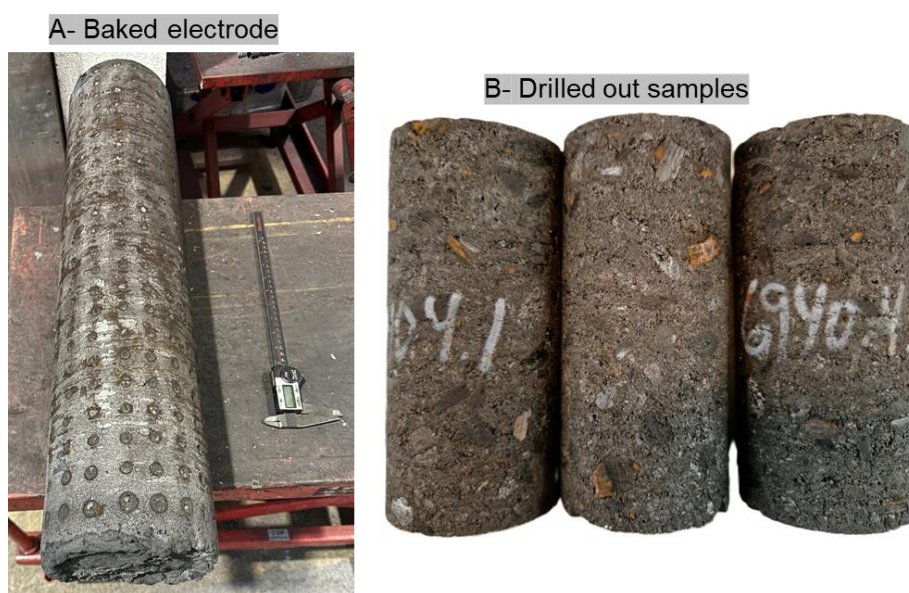


Figure 25. SPL-based baked electrode.

3.2.3. Properties of baked electrode

Density, porosity and permeability

SPL and CTP-based baked electrodes were cut then machined to the required dimensions for each test. Green and baked apparent densities were determined using the standard method ASTM D5502-00.

Hydrostatic density and open porosity were measured based on Archimedes principle and following ISO 12985-2 standard. These techniques can be used to determine the volume fraction of pores that are accessible from the sample surface. Air permeability reflects the internal porosity in the bulk of baked electrode samples. It was measured based on ISO 15906 standard.

Figure 26 shows the baked apparent density of the reference and the test electrodes. SPL has significantly lower coking value compared to CTP (**Table 4**). Furthermore, SPL-based paste has significantly more binder content compared to CTP-based paste. Based on these two factors, one would expect lower BAD and higher porosity for the SPL electrode. However, slow baking and probably shrinkage likely compensated, yielding BAD and porosity similar to CTP electrode (**Table 8**). Comparable air permeability indicates similar connected pore networks in the bulk.

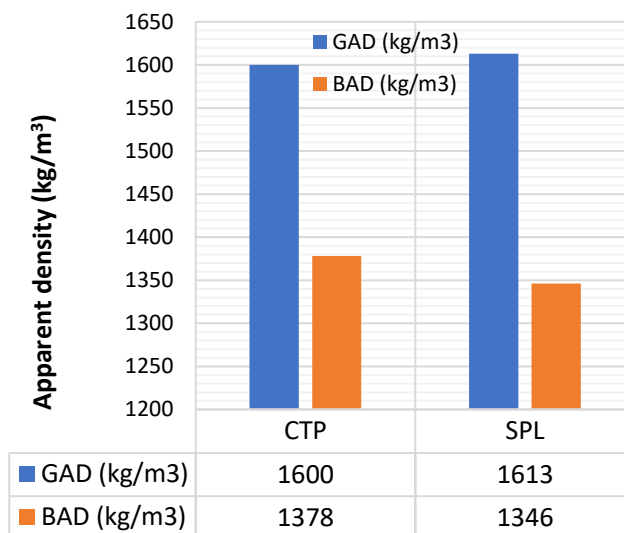


Figure 26. Baked apparent density of SPL and CTP-based electrodes.

Table 8. Open porosity and air permeability of SPL and CTP-based baked electrodes.

Parameter	CTP-electrode	SPL-electrode
Open porosity, %	27	28
Air permeability, nPm	18.3	18.0

Mechanical properties

Electrodes are subjected to mechanical stress due to their movement and from materials moving around them during furnace operations. In addition, electrodes also experience severe thermal stresses from sudden temperature changes during critical situations such as furnace shut down or rapid electrode current changes. Under these circumstances, parts of the electrode heat up or cool down at different rates, the carbon cannot expand or shrink freely, which induces internal tensile and compressive stresses. Severe thermally induced mechanical stresses result in electrode breakage. Therefore, electrodes that are mechanically strong and yet flexible are less likely to break due to thermal stress.

Compressive strength (the maximum applied stress on the stress–strain curve) was measured according to ISO 18515. Bending strength was measured based on ISO 12986-2 standard. **Table 9** compares the mechanical characteristics of both SPL and CTP-based electrodes. Compressive strength of both CTP and SPL electrodes is similar. This proves the ability of carbonized SPL to form effective load-bearing bridges (with minimum imperfections) between the coarse anthracite particles during the electrode baking process.

Despite its good compressive strength, SPL electrode is much weaker when subjected to bending stress. High elasticity modulus indicates stiffness or brittleness of the baked SPL electrode. Low bending strength of the SPL electrodes could be due to amorphous nature of carbonized SPL, which could create more brittle binder matrix between the coarser anthracite particles. It is important to verify the wettability of both anthracite and coke with SPL.

Table 9. Mechanical properties of SPL and CTP-based baked electrodes.

Parameter	CTP-electrode	SPL-electrode
Compressive strength, MPa	17.4	17.9
Bending strength, MPa	3.6	2.8
Y-modulus vending, GPa	2.5	2.7

SPL electrodes are expected to have low thermal shock resistance. Operationally, these electrodes may require careful control of thermal transients (e.g., during furnace start-up/shutdown) to avoid flexural failure.

Electrical and thermal properties

The specific electrical resistivity and thermal conductivity of baked electrodes are sensitive to the intrinsic electrical and thermal conductivities of the dry aggregates and the baked binder as well as sample's defects. Electrical resistivity was measured according to an Elkem internal standard. Electric current passes through the sample and the voltage drop were measured with pins mounted on sample

holder. Thermal conductivity was measured using the hot disk technique, following ISO 22007-2 standard.

Results of electrical resistivity measurements are presented in **Table 10**. Slightly higher electrical resistivity for SPL is consistent with more amorphous, less crystalline carbonized binder and potential microdefects. Yet the overall network conductivity remains similar because aggregate-to-aggregate contacts dominate conduction when the binder maintains continuity.

The similar thermal conductivity of SPL and CTP electrodes (**Table 10**) suggests the composite's effective energy transport is governed by aggregate packing and contact quality more than micro crystallinity of baked binder, and that slow baking preserved contact integrity.

Table 10. Electrical resistivity and thermal conductivity of CTP- and SPL-based baked electrodes.

Parameter	CTP-electrode	SPL-electrode
Electrical resistivity, $\mu\Omega\text{m}$	75.0	80.1
Thermal conductivity, W/mK	3.4	3.5

Air and CO₂ reactivity

In furnace operations at elevated temperatures, electrodes are vulnerable to oxidative gases. Air and CO₂ reactivity of carbon materials is highly affected by their chemical compositions, degree of crystallinity, surface area and the presence of the porosity. High reactivity increases electrode consumption, which increases both production cost and carbon footprint of the metallurgical operation.

Reactivity of baked electrodes against air and CO₂ were measured according to ISO 12989-1 and ISO 12988-1 standards, respectively. The electrode sample was heated to targeted temperature under flowing N₂. Once the desired temperature was achieved, the inert gas was replaced by oxidative gas. Finally, the reaction was stopped and sample cooled down to the room temperature under continuous N₂ flow.

The tested sample was collected from the furnace and loose carbon particles of the residual electrode body were removed and the weight of residual electrode was recorded. The air reactivity residue (ARR), and CO₂ reactivity residue (CRR) were calculated based on the initial mass of the test sample. High ARR and CRR mean low electrode reactivity against oxidative gas.

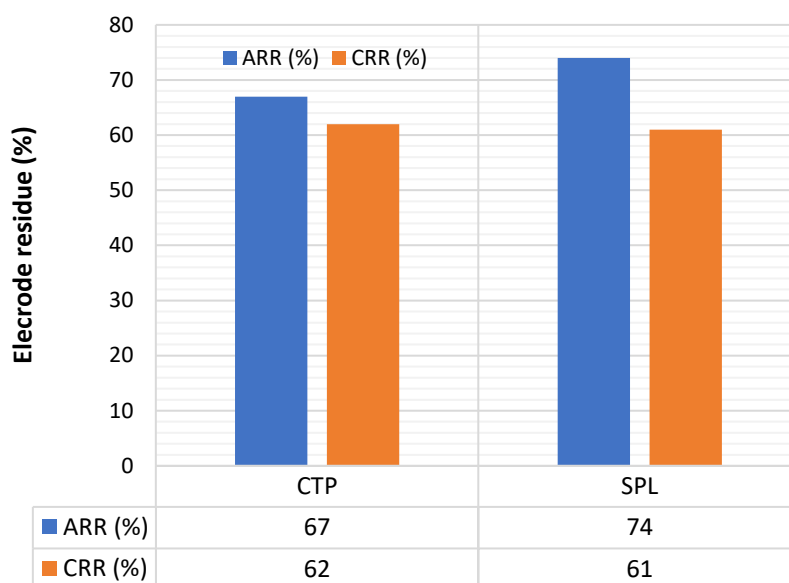


Figure 27. ARR and CRR of SPL and CTP-based baked electrodes.

Figure 27 shows the ARR and CRR of both SPL and CTP electrodes. Carbonized SPL has less ordered carbon structure compared to carbonized CTP. It means the carbonized SPL is expected to be more reactive against air and CO₂, a trend also observed in the air reactivity tests performed by TGA (**Figure 11**). Surprisingly, SPL-electrodes show similar or even better resistance to oxidative gases at high temperatures, a behavior also suggested by the CO₂ reactivity measured by TGA (**Figure 12**). The adjusted baking schedule might reduce accessible reactive surface and reduce the overall reactivity.

3.3. Summary and conclusions on the application of pyrolytic lignin in the manufacture of bio-based Söderberg electrode pastes

In this work package, the suitability of Solid Pyrolytic Lignin (SPL) as a renewable binder for Söderberg electrodes is evaluated. SPL has a narrower and lower-temperature plasticity window than coal tar pitch, and its thermal instability leads to a sharp increase in viscosity above 170 °C due to condensation and crosslinking reactions. For this reason, rigorous temperature control during binder–aggregate mixing is required, making its direct use in Söderberg electrode paste manufacturing challenging. At typical CTP plasticity conditions (~300 °C), SPL melts, rapidly devolatilizes, and carbonizes prematurely, risking segregation and incomplete filling. Therefore, SPL electrodes must be baked at slower slip rates to mitigate foaming, cracking, and porosity.

Despite lower coking value and lack of QI, SPL binder can form continuous, load-bearing bridges between aggregates, producing compressive strength, and thermal and electrical properties comparable to CTP. The SPL binder matrix is stiffer and more brittle, yielding lower flexural strength; this is consistent with its amorphous carbon character that normally toughens CTP-derived matrices.

Overall, SPL binder does not meet the flow requirements needed for Söderberg electrode use. For industrial application of this binder, the TCF process must be adjusted to produce a binder with reduced odor, thermal stability up to 200–300 °C to prevent premature devolatilization and carbonization and controlled thermo-viscous behavior that ensures consistent viscosity during aggregate mixing while preventing undesired self-polymerization. With these characteristics, SPL could achieve performance comparable to CTP in key metrics such as absolute density, rheological behavior, coking value, and carbonization performance, making it a viable alternative for industrial Söderberg electrode production.

Although SPL does not seem feasible to use as direct substitute in Söderberg electrode paste products, this does not necessarily preclude its use in statically-formed industrial electrode products as carbon anodes for electrolytic aluminium reduction, and pre-baked carbon electrodes. Thermo-mechanical strength, air reactivity, and electrical properties may be adequate for these other applications with SPL-based binders. Production of such products with SPL could be feasible since baking heating rates are very slow in these production processes.

3.4. Testing of solid pyrolytic lignin as bio-binder of refractory bricks

Intocast Iberica accepted in November of 2022 collaborating in Bio-Binders project as industrial partner. Aim of this collaboration was supporting the evaluation of new pitch-like bio binders as alternative to pitch in carbon bonded refractory bricks.

Intocast Iberica is part of the Intocast Group in which several plants use pitch as carbon binder for different refractory bricks:

- Oberhausen Plant (GER) – Mg-C pitch bonded bricks (see **Figure 28**)
- Dolomite Franchi (ITA) – Doloma-carbon pitch bonded bricks

Intocast Iberica R&D facilities can carry out different laboratory and industrial testing using pitch but the reason to be integrated in the current project is the closed relationship with KTH team leading the project.

Two pitch alternatives have been provided by BTG during the project, to be promoted as refractory binders, solid and liquid pyrolytic lignins. Batches of both types were manufactured by BTG and sent to Intocast Iberica for testing.

3.4.1. Process of manufacturing pitch-bonded refractory bricks

Manufacturing pitch-bonded refractory bricks involves certain special steps regarding paste mixing. Melting point of coal tar pitch is close to 100-130 °C, so hot mixing is necessary. Summary of mixing steps is as follows:

- Pitch is stored liquid in an appropriate deposit.
- Coarse fraction of the mineral composition is heated through a trommel equipped with a gas burner, before loaded to the mixer.
- Once this preheated coarse fraction has been added to the mixer (see **Figure 29**), pitch fraction is pumped on top and mixed for several minutes.
- Next step is adding mineral powder fraction and graphite, mixing for a longer step of 10-20 minutes until reaching proper pressing ability.
- Once the paste is finished, it is immediately transferred to the press because there is a temperature gap for optimum compaction.

After bricks pressing have been finished, a tempering step of 300-350 °C is necessary to release main volatiles, as well as developing maximum strength of pitch carbonaceous matrix.

For laboratory testing of pitch alternatives, Dolomite Franchi plant in Italy was selected, because they have a special laboratory mixer able to operate mixing in hot state, so industrial proceeding reproduction is closer than rest of Intocast plants. In addition to the latter, Italian R&D Team is the most expert carrying out such type of laboratory homologation steps with different pitch samples from the market.



Figure 28. Intocast pressing process of hot pitch bonded paste in Oberhausen plant to produce magnesia-carbon bricks.

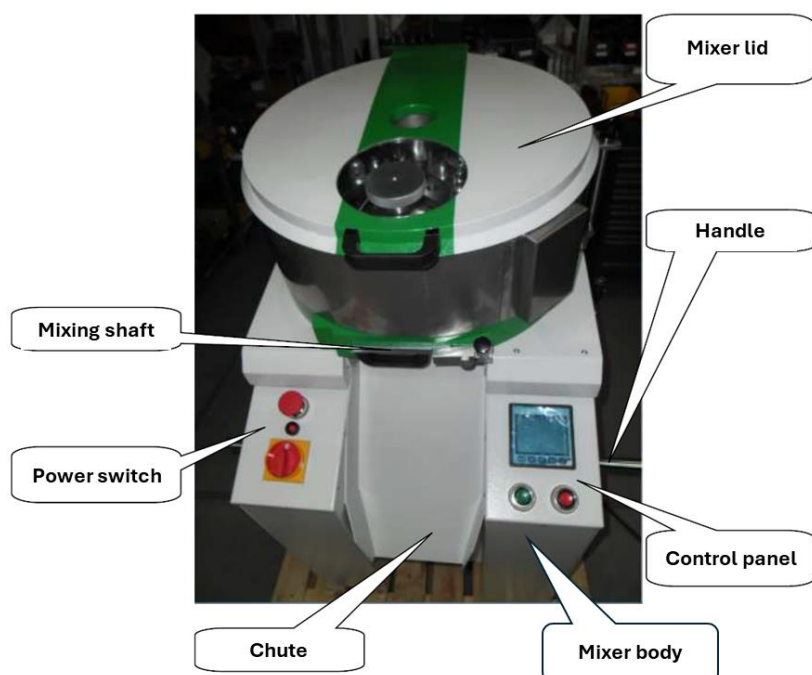


Figure 29. Hot laboratory mixer.

3.4.2. Laboratory testing of solid pyrolytic lignin

Preliminary trials with solid pyrolytic lignin carried out by Intocast experts in Italy showed a narrow gap between melting and boiling, so it seemed not so easy to reach the proper liquid rheology for mineral fraction impregnation under standard procedures.

It is mandatory to determine liquid binder viscosity, previously to mix. With current solid lignin it was not possible to be below 170 °C; at this temperature, binder started to boil.

Even with this drawback, the team tried a mixture of pitch bonded doloma following standard steps:

- Coarse preheating to 170 °C, binder limit.
- Hot lignin addition (7 %) and mixing for 5 minutes.
- Mineral fines addition and mixing for 15 minutes.

Unfortunately, it was not possible to get a proper mixing paste to be pressed, see **Figure 30**. Some other preheating condition of the minerals derives in lignin solidification, see **Figure 31**, so testing conclusion was solid pyrolytic lignin could not be considered as refractory carbonaceous binder.



Figure 30. Paste mixed under standard conditions.



Figure 31. Paste mixed under ‘special’ conditions.

3.4.3. Laboratory testing of liquid pyrolytic lignin

Two types of liquid lignin were provided by BTG, a standard with enough water content to hydrate doloma and a water-free version, especially manufactured for doloma binding. The latter was the only one used by Intocast Italian R&D Team.

Initial study of lignin rheology indicated an operating temperature interval between 80-90 °C; after 80 °C there is a strong decrease in liquid viscosity which enables mixing procedure. Boiling starts at 90 °C, fixing the maximum achievable temperature.

Table 11 presents the collection of different trials, including final density of laboratory pressed 80x80mm cylinders, as well as cold crushing strength values.

Figure 32 shows paste appearance of trial 6, a proper semidry standard paste.



Figure 32. Paste corresponding to trial 6.

Table 11. Summary of properties of tested refractory brick samples.

Mix no.	Binder type	Content (%)	Sample	Bulk density (g/cm ³)	Cold crushing strength (MPa)	Comments
1	LPL	7.04	– – –	– – –	– – –	Doloma hydrated
2	LPL	6.93	– – –	– – –	– – –	Doloma hydrated
3	SPL	9.24	3A 3B 3C	2.575 2.544 –	37.4 – –	Paste humid in excess
4	SPL	6.97	4A 4B 4C	2.667 2.631 2.609	48.5 – –	Normal
5	SPL	8.04	5A 5B 5C	2.572 2.543 2.510	33.3 – –	Cracks after tempering
6	SPL	7.66	6A 6B 6C	2.601 2.579 2.546	38.5 – –	Normal
7	SPL	8.11	7A 7B 7C	2.847 2.761 2.671	67.1 – 43.0	Normal
8	SPL	7.37	8A 8B 8C	2.833 2.830 2.686	– 54.1 57.2	Final paste too cold, low workability

2026-201629-0001 2026-02-04

Based on the work carried out by Intocast, the following conclusions can be drawn:

- Solid pyrolytic lignin (SPL) could not act as carbonaceous binder of refractory bricks.
- Liquid pyrolytic lignin (LPL) allowed the laboratory manufacturing of refractory bricks.
- Narrow gap between 80-90 °C will not allow the use of LPL at industrial scale due to the thermal loss during standard plant process. Additional improvements in current LPL should be necessary to reach a real candidate to substitute coal tar pitch as refractory binder.

4. Work package 4: Evaluation of scale-up and economic analyses of bio-carbon electrodes for metallurgy and steelmaking applications

4.1. Conceptual design and flowsheets

Figure 33 illustrates the integration of fast pyrolysis of lignocellulosic biomass, fractionation of the resulting bio-oil, and the formation of bio-carbon electrode paste using solid pyrolytic lignin as a binder. The lignocellulosic biomass feedstock—specifically woody biomass—is first size-reduced. Prior to feeding, the sized biomass undergoes a drying step to remove adsorbed moisture, thereby reducing the auxiliary energy required to maintain the pyrolysis reactor at its operating temperature.

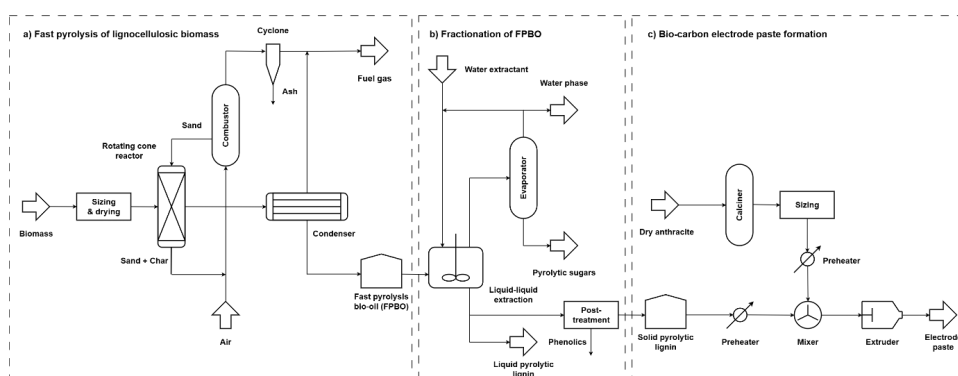


Figure 33. Flowsheet for the bio-carbon electrode formation process from lignocellulosic biomass. (A larger version is included in the Appendix)

The thermochemical conversion of biomass is carried out in a rotating cone reactor (**Figure 33a**), selected for its excellent heat transfer performance and uniform temperature distribution between solid particles (e.g. softwood sawdust and sand). Fast pyrolysis is performed in an inert atmosphere under short vapor residence times (<10 s) to maximize the production of bio-oil. The pyrolysis vapors formed in the process are rapidly directed to a condensation unit, where the vapors are cooled and condensed into a liquid product, the pyrolysis oil. Pyrolysis oil is thus the primary product of the process, reaching a maximum of approximately 70% of the total yield. About 15 % of the biomass is converted to non-condensable gases which are burned to produce energy.

The solid residue, referred to as biochar and accounting for approximately 15% of the total yield, is conveyed to a fluidized bed combustor along with the inert sand, which serves as the fluidizing medium. In this unit, the biochar is burned, and the regenerated/reheated clean sand is recirculated to the rotating cone reactor. Fly ash particles are removed using a cyclone separator. The process is energetically self-sufficient due to the combustion of non-condensable gases and bio-char.

Fast pyrolysis oil is a complex mixture of organic compounds that can be separated based on their solubility in specific solvents, allowing for effective separation by chemical functionality. The process developed by BTG involves separation based

on liquid–liquid extraction (**Figure 33b**). The combination of fast pyrolysis of biomass followed by oil separation by extraction is called Thermo-Chemical Fractionation (TCF) [22].

A water-based extractant is employed to separate the sugar-derived aqueous fraction from the lignin-derived organic fraction. Pyrolytic sugars (typically representing 35–40 wt.% of the raw pyrolysis oil) are concentrated via evaporation. If adequately purified, the water-based extractant can be recovered and recycled back to the liquid–liquid extraction unit, thereby improving process efficiency and reducing solvent consumption.

The lignin-rich organic phase, referred to as pyrolytic lignin, is divided into two streams. One portion undergoes post-treatment, which includes, among other operations, the separation of phenolic compounds (5 wt.%) and removal of residual moisture, yielding a solid pyrolytic lignin fraction (20–25 wt.%). The remaining portion is retained in liquid form (25–30 wt.%). These two lignin-derived fractions exhibit distinct applications: liquid pyrolytic lignin can be utilized in ramming paste formulations, whereas solid pyrolytic lignin serves as a precursor in bio-carbon electrode paste formation. The present schematic diagram focuses specifically on the latter pathway—the production of bio-carbon electrode paste from solid pyrolytic lignin.

The novelty of this project lies in the production of carbon Söderberg electrode paste using a bio-based binder (**Figure 33c**). Solid pyrolytic lignin has shown potential for direct use in the Söderberg electrode paste formation process; however, certain properties, such as low coking value and thermal stability, need improvement to enable industrial-scale feasibility. Ideally, the solid pyrolytic lignin is preheated before being mixed with the fossil-carbon aggregate, in this case, dry anthracite, which has previously been carbonized/graphitized in an electrical calciner, losing approximately 15% of its original mass, and then classified into three size fractions (fine, intermediate, and coarse). During the mixing stage, the three aggregate fractions and the binder are combined in a heated mixer to reduce the binder’s viscosity and enhance its wetting of the aggregate surfaces. The resulting fluid paste is then compacted, molded, and extruded into briquettes, which are subsequently cooled, packaged, and delivered to the client.

4.2. Mass balances

Based on the process flow diagram, a material balance was carried out for an integrated plant combining thermochemical fractionation of biomass and bio-carbon electrode paste production, with an annual capacity of 60 000 t/year of Söderberg electrode paste, representative of existing Elkem Carbon facilities. The plant capacity was estimated based on six anthracite calcination furnaces, which provide sufficient anthracite material to produce 10,000 t/year of carbon electrode paste. Preliminary mass balances (**Table 12**) were performed for the main process units, considering primary raw materials, main products, and by-products, while

auxiliary inputs and outputs such as utilities, solvents, and secondary by-products were excluded. An initial calculation basis of 1 000 kg/h of electrode paste was defined and scaled to the actual production capacity of 7 500 kg/h, assuming 8 000 h/year of effective operation, with all data expressed in kg/h to facilitate the analysis.

Table 12. Simplified mass balances of an integrated plant combining thermochemical fractionation of biomass and bio-carbon electrode paste production.

a) Fast pyrolysis of biomass (rotating cone reactor)					
Inlet streams	wt.%	kg/h	Outlet streams	wt.%	kg/h
Biomass	100	12 000	Non-condensable gases	15	1 800
			FPBO	70	8 400
			Bio-char	15	1 800
b) Fractionation of FPBO					
Inlet streams	wt.%	kg/h	Outlet streams	wt.%	kg/h
FPBO	100	8 400	LS	40	3 360
			LPL	30	2 520
			Phenolics	5	420
			SPL	25	2 100
c) Bio-carbon electrode paste formation					
Inlet streams	wt.%	kg/h	Outlet streams	wt.%	kg/h
SPL	100	2 100	Electrode paste	100	7 500
Dry anthracite	100	6 353			

4.3. Techno-economic analysis

Notably, the economic data used in this assessment are based on estimations and publicly available sources rather than being provided by BTG. In this context, a techno-economic analysis of the thermochemical biomass fractionation process is performed to estimate the selling price of solid pyrolytic lignin and assess its economic feasibility. The selling price (3) is determined based on the unit production cost, calculated as the operating expenditure (OPEX) divided by the process production capacity, and applying an assumed profit margin.

$$\text{Selling price} \left(\frac{\text{SEK}}{t} \right) = \frac{\text{OPEX (SEK/y)}}{\text{Production capacity (t/y)}} \cdot (1 + \text{profit margin}) \quad (3)$$

Unit production cost (SEK/t)

To evaluate the economic feasibility of the project, a first-order cash flow analysis is conducted, considering only process inflows (revenues) and outflows (OPEX). In this techno-economic analysis (TEA), the initial investment is represented by the Capital Expenditure (CAPEX) of the thermochemical biomass fractionation process, including both biomass fast pyrolysis and the subsequent bio-oil fractionation stages.

4.3.1. Estimation of CAPEX

For the estimation of CAPEX, two different methodologies were applied to the distinct parts of the TCF process. On the one hand, for the fast pyrolysis of lignocellulosic biomass, a well-established technology, CAPEX was preliminarily estimated based on a reference biomass pyrolysis plant with known investment cost (see **Table 13**) and scaled to the current process capacity using the Williams formula (4) [46].

$$\text{Williams formula: } C_{P,adj} \text{ (MSEK)} = C_R \cdot \left(\frac{Q_P}{Q_R}\right)^n \cdot \frac{CEPCI_t}{CEPCI_r} \cdot ER \quad (4)$$

In this equation:

- $C_{P,adj}$: Adjusted plant cost in the target year and currency
- C_R : Base cost of the reference plant (base year and currency)
- Q_P : Capacity of the proposed plant
- Q_R : Capacity of the reference plant
- n : Scaling exponent (typical value for chemical plants: 0.6)
- $CEPCI_t$: Chemical Engineering Plant Cost Index for the target year [47]
- $CEPCI_r$: Chemical Engineering Plant Cost Index for the base year [47]
- ER : Exchange rate (target currency / base currency)

Table 13. Empyro plant by BTG Bioliquids BV in Hengelo, the Netherlands [48].

Category	Details
Feedstock	Woody biomass
Products	Fast pyrolysis bio-oil (FPBO), electricity and steam
Production capacity	5 t/h dry feedstock (~25 MW input)
Energy input	Self-sustaining (no external energy input)
Investment cost	20 M€ (2014 price level)

On the other hand, for the fractionation of FPBO, the total CAPEX was estimated for the two main pieces of equipment in this section—the liquid–liquid extraction and evaporation units—by applying the Lang factor method (5) [46]. These units were sized and priced following *Chemical Engineering Design* by Towler and Sinnott, with their capacities used as the design variables (see **Table 14**).

$$\text{Lang factor method: } C_{plant} \text{ (MSEK)} = f_L \cdot \sum f_{material} \cdot C_{equipment} \cdot ER \quad (5)$$

In this equation:

- C_{plant} : total plant cost (capital investment)
- $C_{\text{equipment}}$: total cost of the major equipment
- f_{material} : construction material factor (typical value for stainless steel SS316: 1.8)
- f_L : Lang factor, dimensionless coefficient accounting for installation, piping, instrumentation, structures, engineering, and contingencies (typical value for liquid processing plants: 5.7)
- ER : Exchange rate (target currency / base currency)

Table 14. Main pieces of equipment used for FPBO fractionation [46]. CSI refers to Commercially Sensitive Information.

Equipment (Carbon steel)	Capacity (t/h)	Base price (SEK)	Thermal energy (kW)	Installed power (kW)
Mixer-settler	CSI	CSI	–	CSI
4-effect evaporator	CSI	CSI	CSI	CSI

4.3.2. Estimation of OPEX

For a simplified estimation of OPEX (6), only the costs of materials, thermal energy, and electricity were considered. Material costs were limited to the raw biomass and the make-up water extractant used for FPBO fractionation. It should be noted that no external energy input was assumed for the fast pyrolysis of softwood sawdust, owing to the self-sustaining operation of the process (see **Table 13**). Conversely, the energy input parameters for the fractionation process are provided in **Table 14**. The remaining parameters for OPEX estimation for both the pyrolysis and fractionation subprocesses are listed in **Table 15**.

$$OPEX \left(\frac{MSEK}{year} \right) = C_{\text{materials}} + C_{\text{thermal}} + C_{\text{electrical}} \quad (6)$$

In this equation:

- OPEX: Total annual operating costs of the plant
- $C_{\text{materials}}$: Cost of materials consumed in the process
- C_{thermal} : Cost of thermal energy used in the process
- $C_{\text{electrical}}$: Cost of electrical energy consumed by the plant

Table 15. Summary of the main process parameters for OPEX calculation. CSI refers to Commercially Sensitive Information.

Parameter	Assumption	Reference
Duration of operation	8000 h/year	–
Raw materials		
Softwood sawdust	500 SEK/t	[49]
Water extractant	9.75 SEK/m ³	[50]
Mixer-settler		
FPBO:water ratio	CSI	–
Water extractant recirculation	CSI	–
Capacity factor	CSI	–
Utilities		
Electricity (SEK/kWh)	2.214	[51]
Natural gas (SEK/kWh)	1.682	[52]

4.3.3. Comparison of CAPEX, OPEX and SPL production costs

The CAPEX and OPEX of the distinct parts of the TCF process were estimated according to the methodologies explained in the previous sections and are gathered in **Table 16**. The results indicate that fast pyrolysis dominates capital investment due to the greater complexity of biomass processing and by-product management. In contrast, FPBO fractionation has a higher impact on operating costs due to the evaporation of the large volume of water extractant, since the biomass pyrolysis is self-sustaining and ideally only incurs material costs.

Table 16. Estimated CAPEX and OPEX for the Thermochemical Fractionation process of biomass. CSI refers to Commercially Sensitive Information.

TCF process step	CAPEX (MSEK)	OPEX (MSEK/year)
Fast pyrolysis of biomass	CSI	CSI
Fractionation of FPBO	CSI	CSI

The selling price of solid pyrolytic lignin was calculated using Equation 3 and compared with that of coal tar pitch, which is currently used by Elkem Carbon, as shown in **Table 17**. Assuming a conservative profit margin of 20 % for both binders, solid pyrolytic lignin demonstrates price competitiveness when used as a binder in the production of Söderberg electrode paste.

Table 17. Comparison of production costs and selling prices of fossil- and bio-based binders, assuming a 20 % profit margin. Selling prices reported in the literature are expressed in \$/t [53]. CSI refers to Commercially Sensitive Information.

Binder	Unit production cost (\$/t)	Unit selling price (\$/t)
Solid pyrolytic lignin	CSI	CSI
Coal tar pitch	672	840

Moreover, a 5 % increase in the binder content of the bio-based electrode paste would positively affect the OPEX of the electrode paste production process (not shown), as the reduced anthracite demand decreases the energy requirement of its most energy-intensive operation, carbonization–graphitization in the calciner, which consumes approximately 1 000 kW per ton [53].

4.3.4. Evaluation of cash flow and profitability

A biomass thermochemical fractionation plant, as described above, is proposed for the production of bio-based Söderberg electrode paste, assuming a 20-year operational lifetime. For a first-order techno-economic analysis, the annual cash flow (7) is defined as the net difference between revenues and operating expenses.

$$\text{Annual cash flow: } CF_t \left(\frac{\text{MSEK}}{\text{year}} \right) = \sum_{t=1}^n (R_t + OPEX_t); \quad t = 1, 2, \dots, 20 \quad (7)$$

In this equation:

- CF_t : cash flow in year t
- R_t : total revenue from products and by-products in year t
- $OPEX_t$: operating expenses in year t

The total revenue (8) from products and by-products was estimated and is summarized in **Table 18**. As mentioned above, a 20 % profit margin was assumed for SPL binder, one of the primary process inputs in the electrode paste production process. For the remaining by-products, the unit selling price was conservatively set at one-third of their production cost to guarantee their complete sales, given the limited market demand for large volumes of chemicals and the additional costs associated with managing surplus or unused by-products.

$$\text{Revenue} \left(\frac{\text{MSEK}}{\text{year}} \right) = \text{Unit selling price} \left(\frac{\text{SEK}}{t} \right) \cdot \text{Production capacity} \left(\frac{t}{\text{year}} \right) \quad (8)$$

Table 18. Estimated revenues for primary products and by-products from the TCF of biomass. CSI refers to Commercially Sensitive Information.

Product/by-product	Unit production cost (SEK/t)	Unit selling price (SEK/t)	Revenue (MSEK/year)
Solid pyrolytic lignin	CSI	CSI	CSI
Liquid pyrolytic lignin	CSI	CSI	CSI
Pyrolytic sugars	CSI	CSI	CSI
Phenolics	CSI	CSI	CSI

The cumulative cash flow (9) represents the net accumulation of cash flows over time, incorporating the initial capital investment (CAPEX) and considering the expected rate of return (ERR) for the project.

$$CF_{cum,t} \text{ (MSEK)} = -CAPEX_{(a+b)} + \sum_{t=1}^n \frac{CF_t}{(1+ERR)^t}; t = 1, 2, \dots, 20 \quad (9)$$

In this equation:

- $CF_{cum,t}$: Cumulative cash flow in year t
- $CAPEX_{(a+b)}$: initial capital investment for biomass fast pyrolysis (a) and FPBO fractionation (b)
- CF_t : annual cash flow in year t
- ERR : expected rate of return

The Internal Rate of Return (IRR) is the discount rate at which the net present value (NPV) of a project becomes zero (10), meaning that the present value of cash inflows equals the initial investment. For this study, the IRR was calculated using the IRR function in Microsoft Excel, which iteratively finds the rate that satisfies $NPV = 0$ based on the projected cash flows over the plant's operational lifetime. This method allows for a reliable estimation of the project's profitability and enables comparison with the hurdle rate to assess financial feasibility.

$$\text{Net present value: } NPV = \sum_{t=1}^n \frac{CF_t}{(1+IRR)^t} - CAPEX_{a+b} = 0 \quad (10)$$

In this equation:

- $CAPEX_{(a+b)}$: initial capital investment for biomass fast pyrolysis (a) and FPBO fractionation (b)
- CF_t : annual cash flow in year t
- IRR : internal rate of return

The results of the cumulative cash flow analysis are presented in **Figure 34**, considering two scenarios characterized by different expected rates of return (ERR): a low ERR of 4 % and a high ERR of 10 %. In both cases, the investment payback period is reached within 4 to 6 years, indicating a favorable economic performance for the proposed TCF plant, as payback periods in the range of 5–7 years are generally considered acceptable.

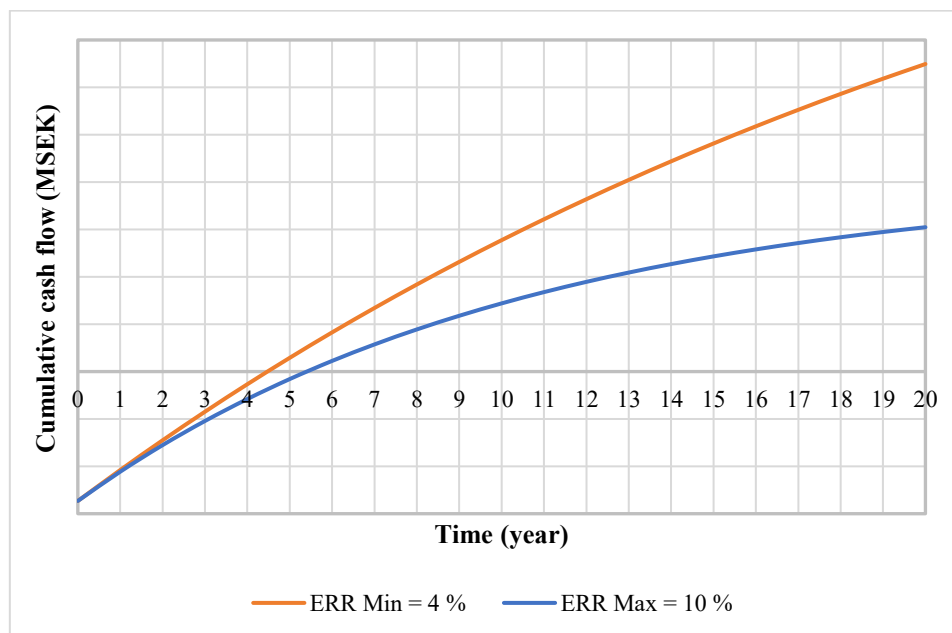


Figure 34. Cumulative discounted cash flow of the TCF plant over 20 years of operation.

In addition, the Internal Rate of Return (IRR) derived from the cumulative cash flow analysis for the two ERR scenarios (not shown) is above the typical hurdle rates reported for similar biomass-based industrial projects (10–12 %), further supporting the economic feasibility of the TCF process.

It should be noted that this evaluation is based on a first-order cash flow analysis, and several simplifying assumptions were applied. Costs associated with maintenance, labor, waste management, taxes and other indirect expenses were not explicitly considered, which may influence the absolute economic indicators. From an optimization perspective, the ideal scenario would be for the plant to be economically sustained solely by the revenue generated from solid pyrolytic lignin (SPL), the primary product of interest. Although this condition is not fully met in the present analysis, several improvement strategies could enhance the overall economic performance of the process. Potential measures to reduce CAPEX include equipment design optimization and improved process integration, while OPEX could be further reduced through enhanced energy integration, decreased solvent consumption, and overall improvements in process efficiency.

4.4. Summary and conclusions on Work Package 4

In summary, from the techno-economic assessment of the proposed TCF process, several key conclusions can be drawn:

- **Competitive production costs:** Based on OPEX estimations and process capacity, solid pyrolytic lignin (SPL) exhibits a production cost comparable to that of coal tar pitch, making it a competitive binder alternative for Söderberg electrode paste production.
- **Economic viability:** The production and sale of solid pyrolytic lignin (SPL) is supported by the calculated Internal Rate of Return (IRR) and exceeds typical hurdle rates for comparable biomass-processing plants, even under a high expected rate of return scenario. Although the plant cannot yet be fully sustained by SPL revenue alone, it contributes substantially to the overall profitability of the process.
- **Operational benefits:** Incorporating a higher concentration of SPL as a binder in the electrode paste production process reduces the thermal energy demand in the manufacture of Söderberg electrode paste, due to the lower anthracite requirements, thereby improving the overall operating costs of the process.

Diskussion

The results of the current project demonstrate that bio-based binders derived from pyrolysis oil—particularly solid pyrolytic lignin and pyrolytic sugar fractions—exhibit strong potential as renewable alternatives to the fossil-based binder coal tar pitch in carbon electrode, lining, and refractory applications. Pilot-scale testing corroborates that these materials provide mechanical, thermal, and electrical performance comparable to fossil-based binders in Söderberg electrode pastes.

However, several factors currently limit the industrial-scale use of these bio-binders. The SPL binder shows: (i) a narrower and lower-temperature plasticity window, which can lead to early melting and carbonization under typical CTP processing conditions, affecting material handling and phase uniformity in electrode pastes; (ii) a rising dynamic viscosity at aggregate–binder mixing temperatures due to self-polymerization reactions; (iii) moderate wettability with conventional carbon aggregates, such as anthracite, which can influence mixing and dispersion in electrode pastes; and (iv) a relatively low graphitizability, mainly due to its oxygen content and structural disorder, which may limit its use in systems requiring a high degree of graphitization, such as graphite and pre-baked electrodes. Targeted adjustments in the TCF process—including optimized fast pyrolysis, thermochemical fractionation, and post-processing via thermal and chemical treatments—together with suitable graphitization catalysts, could yield a binder with enhanced thermophysical properties, superior thermal stability, and improved graphitizability for Söderberg electrode pastes.

Catalytic graphitization experiments show that the addition of fine reduced Fe powder enhances the structural ordering of the carbon network in SPL during thermal treatment. While full graphitization was not achieved at 1100–1300 °C, the level attained may already be sufficient for Söderberg electrode applications. Higher temperatures (~2000 °C) can enable near-complete graphitization, with catalyst content optimized to preserve desirable binder thermophysical properties and facilitate subsequent processing steps. Importantly, when maintained at low concentrations, iron catalysts do not compromise the quality of ferroalloys produced in SAFs using Söderberg self-baking electrodes. Consequently, the development and application of bio-based Fe-containing Söderberg electrode pastes will be explored as a promising subject for future research projects.

Graphene oxide is a promising graphitization catalyst, as its compositional similarity to graphite eliminates the need for post-treatment removal. However, the heterogeneous nature of SPL limits effective crosslinking with the catalyst. Therefore, optimization of the TCF process should also aim to produce a tailored, more homogeneous SPL composition, enhancing catalyst–binder interactions and improving the efficiency of graphene oxide-induced graphitization.

Results interpretation through an energy systems lens

From an energy systems perspective, these findings are highly relevant, as integrating bio-based binders into industrial carbon electrode production can directly reduce reliance on CTP and other fossil carbon-derived binders, whose extraction and processing require substantial energy inputs. Lignocellulosic biomass is an abundant and readily available feedstock. Although it requires further processing to function as a binder, the thermochemical fractionation (TCF) process proposed by BTG Biomass Technology is particularly energy-efficient, with pyrolysis generating an energy surplus through the combustion of solid and gaseous by-products, rendering this process unit self-sustaining. Additionally, the incorporation of suitable graphitization catalysts can enhance the structural ordering of the carbon network within the electrode, improving electrical conductivity and thermal properties. Enhanced graphitization facilitates more efficient heat transfer and charge transport, potentially reducing overall energy consumption during electrode operation.

Altogether, optimized bio-binders and sustainable catalyst systems provide a pathway to lowering the environmental impact of fossil-based binders and promoting more energy-efficient decarbonization in the metallurgical and steel sectors. Furthermore, valorizing lignocellulosic residues strengthens the integration of Sweden's forestry, bioenergy, and metallurgical industries, supporting a transition toward a more circular and resource-efficient industrial ecosystem.

Future work

To fully realize the potential of bio-based binders in metallurgical applications, several critical research and development steps should be prioritized:

1. Optimization of biomass conversion processes for binder upgrading
 - Refinement of fast pyrolysis and thermochemical fractionation conditions.
 - Implementation of thermal and/or chemical post-treatments to reduce odor, enhance thermal stability, broaden the plasticity window, ensure consistent viscosity during aggregate-binder mixing, and improve compositional uniformity.

2026-02-04

2026-201629-0001

2. Novel approaches for enhanced graphitization and catalyst removal
 - Further investigation of sustainable catalytic systems, including Fe⁰-based and structured carbon-based catalysts, such as graphene oxide.
 - Exploration of efficient approaches for removing catalyst residues, and/or identification of catalysts that do not require post-reaction removal.
3. Further pilot-scale validation
 - Preparation of Söderberg electrode prototypes using optimized bio-binder formulations and catalyst-containing bio-binder blends.
 - Assessment of mechanical integrity, thermal behavior, and electrical conductivity under relevant operating conditions.
 - Testing of application of SPL binders for direct application in carbon anode production for Al smelting.
4. Holistic sustainability and techno-economic analysis
 - Quantification of the environmental impact of bio-binder application through life-cycle analysis, including determination of greenhouse gas savings.
 - More comprehensive techno-economic evaluation of production costs, supply chain integration, and large-scale feasibility.

Expected societal impacts

The outcomes of this research are expected to generate several long-term societal benefits. The replacement of fossil-based binders with renewable alternatives supports national climate and energy objectives, contributing to reduced carbon emissions and enhanced circularity in resource use. The valorization of forestry and bioenergy residues adds economic value to regional biomass streams, strengthening rural economies and supporting Sweden's bio-based industrial strategy. Furthermore, the development of expertise in advanced bio-carbon materials cultivates a skilled workforce and reinforces Sweden's leadership in sustainable materials innovation. As the solutions developed in this project are scalable and transferable, they offer broader international relevance and can contribute to global efforts toward decarbonizing energy-intensive industries.

Publikationslista

Published articles:

- J. White, L.M. López-Renau, B. Glaser, *A Review of Biocarbon Substitutes in Electrodes and Refractories for the Metallurgical Industries*. *Journal of Sustainable Metallurgy* 10 (2024) 1051–1069, DOI: 10.1007/s40831-024-00870-x [54]

Short description of the work: Comprehensive review of the state of the art of bio-based carbon carriers for carbon electrode manufacturing. The article examines current fossil-based carbon carriers used across various electrode industrial applications, evaluates potential bio-based aggregates and binders that can serve as substitutes, and discusses the main challenges associated with their implementation, particularly the low graphitizability of these hard carbons.

Upcoming articles:

- *Role of Reduced Iron Powder in the Catalytic Graphitization of Pyrolytic Lignin* (in preparation)

Short description of the work: This study investigates the graphitizability of pyrolytic lignin upon incorporation of reduced iron powder via physical hot mixing, examining the effects of graphitization temperature and iron catalyst concentration as key variables.

- *Pyrolytic Lignin as a Sustainable Binder for Bio-Based Söderberg Electrode Pastes* (in preparation)

Short description of the work: This study evaluates the feasibility of bio-carbon Söderberg electrode prototypes incorporating pyrolytic lignin as a binder, by comparing their critical properties with those of electrodes produced using fossil-derived coal tar pitch conventionally employed in metallurgical and steelmaking applications.

Referenser, källor

- [1] European Commission, “Critical Raw Materials Resilience: Charting a Path towards greater Security and Sustainability, COM/2020/474, Document 52020DC0474,” 2020.
- [2] Market Data Forecast, “Europe Graphite Market Size, Share, Trends & Growth Forecast Report,” 2025. Accessed: Jan. 26, 2026. [Online]. Available: <https://www.marketdataforecast.com/market-reports/europe-graphite-market>
- [3] H. Marsh and F. Rodríguez-Reinoso, *Sciences of Carbon Materials*. Universidad de Alicante, 2000.
- [4] R. J. Gray and K. C. Krupinski, “Pitch Production: Supply, Coking, Optical Microscopy and Applications,” in *Introduction to Carbon Technologies*, H. Marsh, E. A. Heintz, and F. Rodríguez-Reinoso, Eds., University of Alicante, 1997, pp. 329–423.
- [5] Scientific Committee on Health and Environmental Risks (SCHER), “Scientific Opinion on the Risk Assessment on Coal Tar Pitch, High Temperature: Human Health Part (CAS no. 65996-93-2),” 2008.
- [6] Y. He, K. C. Zhou, Y. Zhang, H. W. Xiong, and L. Zhang, “Recent Progress of Inert Anodes for Carbon-Free Aluminium Electrolysis: A Review and Outlook,” *J. Mater. Chem. A Mater.*, vol. 9, no. 45, pp. 25272–25285, Nov. 2021, doi: 10.1039/D1TA07198J.
- [7] C. W. Söderberg, “Electrode for Electric Furnaces and Process for Manufacturing the Same,” US1440724A, 1923 Accessed: Jan. 22, 2026. [Online]. Available: <https://patents.google.com/patent/US1440724A/en>
- [8] L. Shoko, J. P. Beukes, and C. A. Strydom, “Determining the Baking Isotherm Temperature of Söderberg Electrodes and Associated Structural Changes,” *Miner. Eng.*, vol. 49, pp. 33–39, Aug. 2013, doi: 10.1016/J.MINENG.2013.04.015.
- [9] B. Larsen, J. P. M. Amaro, S. Z. Nascimento, K. Fidje, and H. Gran, “Melting and Densification of Electrode Paste Briquettes in Söderberg Electrodes,” *10th International Ferroalloys Congress*, 2004.
- [10] M. W. Meier, “Cracking Behaviour of Prebaked Carbon Anodes Used for the Aluminium Production,” ETH Zürich, 1995.
- [11] T. Zhu, Y. Li, S. Sang, and Z. Xie, “A New Approach to Fabricate MgO-C Refractories with High Thermal Shock Resistance by Adding Artificial Graphite,” *J. Eur. Ceram. Soc.*, vol. 38, no. 4, pp. 2179–2185, Apr. 2018, doi: 10.1016/J.JEURCERAMSOC.2017.10.018.

2026-02-04

2026-201629-0001

- [12] A. Hussein, M. Fafard, D. Ziegler, and H. Alamdari, "Effects of Charcoal Addition on the Properties of Carbon Anodes," *Metals (Basel)*, vol. 7, no. 3, p. 98, Mar. 2017, doi: 10.3390/MET7030098.
- [13] A. Hussein, F. Larachi, D. Ziegler, and H. Alamdari, "Effects of Heat Treatment and Acid Washing on Properties and Reactivity of Charcoal," *Biomass Bioenergy*, vol. 90, pp. 101–113, Jul. 2016, doi: 10.1016/J.BIOMBIOE.2016.03.041.
- [14] A. Oya and H. Marsh, "Review Phenomena of Catalytic Graphitization," *J. Mater. Sci.*, vol. 17, pp. 309–322, 1982.
- [15] S. I. Talabi, A. P. da Luz, V. C. Pandolfelli, V. H. Lima, V. R. Botaro, and A. de Almeida Lucas, "Graphitization of Lignin-Phenol-Formaldehyde Resins," *Materials Research*, vol. 23, no. 2, 2020, doi: 10.1590/1980-5373-MR-2019-0686.
- [16] A. Effendi, H. Gerhauser, and A. V. Bridgwater, "Production of Renewable Phenolic Resins by Thermochemical Conversion of Biomass: A Review," *Renewable and Sustainable Energy Reviews*, vol. 12, no. 8, pp. 2092–2116, Oct. 2008, doi: 10.1016/J.RSER.2007.04.008.
- [17] J. D. Rocha, A. R. Coutinho, and C. A. Luengo, "Bio-Pitch Produced from Eucalyptus Wood Pyrolysis Liquids as a Renewable Binder for Carbon Electrode Manufacture," *Brazilian Journal of Chemical Engineering*, vol. 19, no. 2, pp. 127–132, 2002, doi: 10.1590/S0104-66322002000200002.
- [18] A. Hussein, Y. Lu, R. Mollaabbasi, J. Tessier, and H. Alamdari, "Bio-Pitch as a Binder in Carbon Anodes for Aluminum Production: Bio-Pitch Properties and its Interaction with Coke Particles," *Fuel*, vol. 275, Sep. 2020, doi: 10.1016/J.FUEL.2020.117875.
- [19] Y. Lu *et al.*, "Properties of Bio-Pitch and its Wettability on Coke," *ACS Sustain. Chem. Eng.*, vol. 8, no. 40, pp. 15366–15374, Oct. 2020, doi: 10.1021/ACSSUSCHEMENG.0C06048.
- [20] Y. Elkasabi, C. A. Mullen, G. D. Strahan, and V. T. Wyatt, "Biobased Tar Pitch Produced from Biomass Pyrolysis Oils," *Fuel*, vol. 318, p. 123300, Jun. 2022, doi: 10.1016/J.FUEL.2022.123300.
- [21] A. Hussein, Z. Wang, A. P. Ratvik, T. Grande, and H. Alamdari, "Electrochemical Performance of Carbon Anodes Made of Bio-pitch as a Binder," *Metallurgical and Materials Transactions B: Process Metallurgy and Materials Processing Science*, vol. 53, no. 1, pp. 584–593, Feb. 2022, doi: 10.1007/S11663-021-02397-Y.
- [22] H. Heeres, E. J. Leijenhurst, R. Ongena, and L. Van De Beld, "Thermal-Chemical Fractionation of Lignocellulosic Biomass," *27th European*

- Biomass Conference and Exhibition*, pp. 1894–1898, 2019, doi: 10.5281/zenodo.3337616.
- [23] M. B. Figueirêdo, I. Hita, P. J. Deuss, R. H. Venderbosch, and H. J. Heeres, “Pyrolytic Lignin: A Promising Biorefinery Feedstock for the Production of Fuels and Valuable Chemicals,” *Green Chemistry*, vol. 24, no. 12, pp. 4680–4702, Jun. 2022, doi: 10.1039/D2GC00302C.
- [24] K. H. Kim, S. Lee, M. Il Kim, and Y. S. Lee, “The Effect of Carbon Black on Reforming of Pyrolysis Fuel Oil for a Binder Pitch,” *Fuel*, vol. 206, pp. 58–63, 2017, doi: 10.1016/j.fuel.2017.05.056.
- [25] X. Huang, D. Kocaefe, Y. Kocaefe, and D. Bhattacharyay, “Wettability of Bio-Coke by Coal Tar Pitch for its Use in Carbon Anodes,” *Colloids Surf. A Physicochem. Eng. Asp.*, vol. 490, pp. 133–144, Feb. 2016, doi: 10.1016/J.COLSURFA.2015.11.044.
- [26] A. Sarkar *et al.*, “Coke–Pitch Interactions during Anode Preparation,” *Fuel*, vol. 117, no. PART A, pp. 598–607, Jan. 2014, doi: 10.1016/J.FUEL.2013.09.015.
- [27] Y. Lu, D. Kocaefe, Y. Kocaefe, X. A. Huang, and D. Bhattacharyay, “The Wettability of Coke by Pitches with Different Quinoline-Insoluble Contents,” *Fuel*, vol. 199, pp. 587–597, Jul. 2017, doi: 10.1016/J.FUEL.2017.03.019.
- [28] W. K. Fischer and R. Perruchoud, “Determining Prebaked Anode Properties for Aluminum Production,” *JOM 1987 39:11*, vol. 39, no. 11, pp. 43–45, Oct. 2012, doi: 10.1007/BF03257539.
- [29] K. Khaji and M. Al Qassemi, “The Role of Anode Manufacturing Processes in Net Carbon Consumption,” *Metals 2016, Vol. 6, Page 128*, vol. 6, no. 6, p. 128, May 2016, doi: 10.3390/MET6060128.
- [30] M. Soltani Hosseini and P. Chartrand, “Thermodynamics and Phase Relationship of Carbonaceous Mesophase Appearing during Coal Tar Pitch Carbonization,” *Fuel*, vol. 275, p. 117899, Sep. 2020, doi: 10.1016/J.FUEL.2020.117899.
- [31] P. Ouzilleau, A. E. Gheribi, G. Eriksson, D. K. Lindberg, and P. Chartrand, “A Size-Dependent Thermodynamic Model for Coke Crystallites: The Carbon–Hydrogen System up to 2500 K,” *Carbon N. Y.*, vol. 85, pp. 99–118, Apr. 2015, doi: 10.1016/J.CARBON.2014.12.042.
- [32] R. E. Franklin, “The structure of graphitic carbons,” *Acta Crystallogr.*, vol. 4, no. 3, pp. 253–261, May 1951, doi: 10.1107/S0365110X51000842.

2026-02-04

2026-201629-0001

- [33] A. L. Patterson, "The Scherrer Formula for X-Ray Particle Size Determination," *Physical Review*, vol. 56, no. 10, p. 978, Nov. 1939, doi: 10.1103/PhysRev.56.978.
- [34] J. Maire and J. Méring, "Graphitization of Soft Carbons," in *Chemistry and Physics of Carbon*, vol. 6, P. L. , Jr. Walker, Ed., New York: Marcel Dekker, 1970, pp. 125–190.
- [35] L. M. Malard, M. A. Pimenta, G. Dresselhaus, and M. S. Dresselhaus, "Raman Spectroscopy in Graphene," *Phys. Rep.*, vol. 473, no. 5–6, pp. 51–87, Apr. 2009, doi: 10.1016/J.PHYSREP.2009.02.003.
- [36] P. J. Yang, T. H. Li, H. Li, A. L. Dang, and L. Yuan, "Progress in the Graphitization and Applications of Modified Resin Carbons," *New Carbon Materials*, vol. 38, no. 1, pp. 96–108, Feb. 2023, doi: 10.1016/S1872-5805(23)60715-2.
- [37] A. S. Kamal, R. Othman, and N. H. Jabarullah., "Preparation and Synthesis of Synthetic Graphite from Biomass Waste: A Review," *Systematic Reviews in Pharmacy*, vol. 11, no. 2, pp. 881–894, 2020, doi: 10.31838/SRP.2020.2.122.
- [38] S. Yi, J. Chen, H. Li, L. Liu, X. Xiao, and X. Zhang, "Effect of Graphite Oxide on Graphitization of Furan Resin Carbon," *Carbon N. Y.*, vol. 48, no. 3, pp. 926–928, Mar. 2010, doi: 10.1016/J.CARBON.2009.11.027.
- [39] S. C. Dey *et al.*, "Catalytic Graphitization of Pyrolysis Oil for Anode Application in Lithium-Ion Batteries," *Green Chemistry*, vol. 26, no. 15, pp. 8840–8853, Jul. 2024, doi: 10.1039/D4GC01647E.
- [40] L. Frankenstein, P. Glomb, J. Ramirez-Rico, M. Winter, T. Placke, and A. Gomez-Martin, "Revealing the Impact of Different Iron-Based Precursors on the 'Catalytic' Graphitization for Synthesis of Anode Materials for Lithium-Ion Batteries," *ChemElectroChem*, vol. 10, no. 5, Mar. 2023, doi: 10.1002/celec.202201073.
- [41] L. Zhao, "Purification of Engineered Graphite for Advanced Application," KTH Royal Institute of Technology, 2022. Accessed: Jan. 22, 2026. [Online]. Available: <https://www.diva-portal.org/smash/record.jsf?pid=diva2%3A1678495&dswid=6910>
- [42] A. Gomez-Martin, Z. Schnepf, and J. Ramirez-Rico, "Structural Evolution in Iron-Catalyzed Graphitization of Hard Carbons," *Chemistry of Materials*, vol. 33, no. 9, pp. 3087–3097, May 2021, doi: 10.1021/ACS.CHEMMATER.0C04385.
- [43] Z. Shi *et al.*, "Catalytic Graphitization of Engineered Pyrolysis Bio-Oil for Sustainable Graphite and Hydrogen Co-Production," *Renew. Energy*, vol. 256, p. 124149, Jan. 2026, doi: 10.1016/J.RENENE.2025.124149.

- [44] S. I. Talabi, A. P. Luz, A. A. Lucas, C. Pagliosa, and V. C. Pandolfelli, "Catalytic Graphitization of Novolac Resin for Refractory Applications," *Ceram. Int.*, vol. 44, no. 4, pp. 3816–3824, Mar. 2018, doi: 10.1016/J.CERAMINT.2017.11.167.
- [45] O. Alizadeh, H. M. Hosseini, A. Pourjavadi, and A. R. Bahramian, "Effect of Graphene Oxide on Morphological and Structural properties of graphene reinforced novolac-derived Carbon Aerogels: A Modified Quasi-Percolation Model," *Ceram. Int.*, vol. 46, no. 8, pp. 11179–11188, Jun. 2020, doi: 10.1016/J.CERAMINT.2020.01.139.
- [46] G. Towler and R. Sinnott, *Chemical Engineering Design: Principles, Practice and Economics of Plant and Process Design (3rd edition)*. Butterworth Heinemann, 2022. Accessed: Jan. 16, 2026. [Online]. Available: <https://www.elsevier.com/books-and-journals>
- [47] W. M. Vatauvuk, "Updating the CE Plant Cost Index," *Chemical Engineering*, pp. 62–70, 2002, Accessed: Jan. 16, 2026. [Online]. Available: https://www.chemengonline.com/Assets/File/CEPCI_2002.pdf
- [48] B. van de Beld, "EMPYRO - Biomass to Pyrolysis Oil," *Best Practices on Flexible Bioenergy*, no. IEA Bioenergy: Task 44, 2024.
- [49] E. Fields, "Exploring Price of Sawdust per Ton: Material Composition, Standards, and Best Practices in Industry." Accessed: Jan. 16, 2026. [Online]. Available: <https://www.alibaba.com/product-insights/price-of-sawdust-per-ton.html>
- [50] I. N. Zaini, N. Sophonrat, K. Sjöblom, and W. Yang, "Creating Values from Biomass Pyrolysis in Sweden: Co-Production of H₂, Biocarbon and Bio-Oil," *Processes*, vol. 9, no. 3, p. 415, Feb. 2021, doi: 10.3390/PR9030415.
- [51] GlobalPetrolPrices.com, "Electricity Prices around the World." Accessed: Jan. 16, 2026. [Online]. Available: https://www.globalpetrolprices.com/electricity_prices/
- [52] GlobalPetrolPrices.com, "Sweden Natural Gas Prices." Accessed: Jan. 16, 2026. [Online]. Available: https://www.globalpetrolprices.com/Sweden/natural_gas_prices/
- [53] A. de Pretto, "Production of Söderberg Electrode Paste," 2025.
- [54] J. F. White, L. M. L. Renau, and B. Glaser, "A Review of Biocarbon Substitutes in Electrodes and Refractories for the Metallurgical Industries," Sep. 01, 2024, *Springer Science and Business Media Deutschland GmbH*. doi: 10.1007/s40831-024-00870-x.

Bilagor

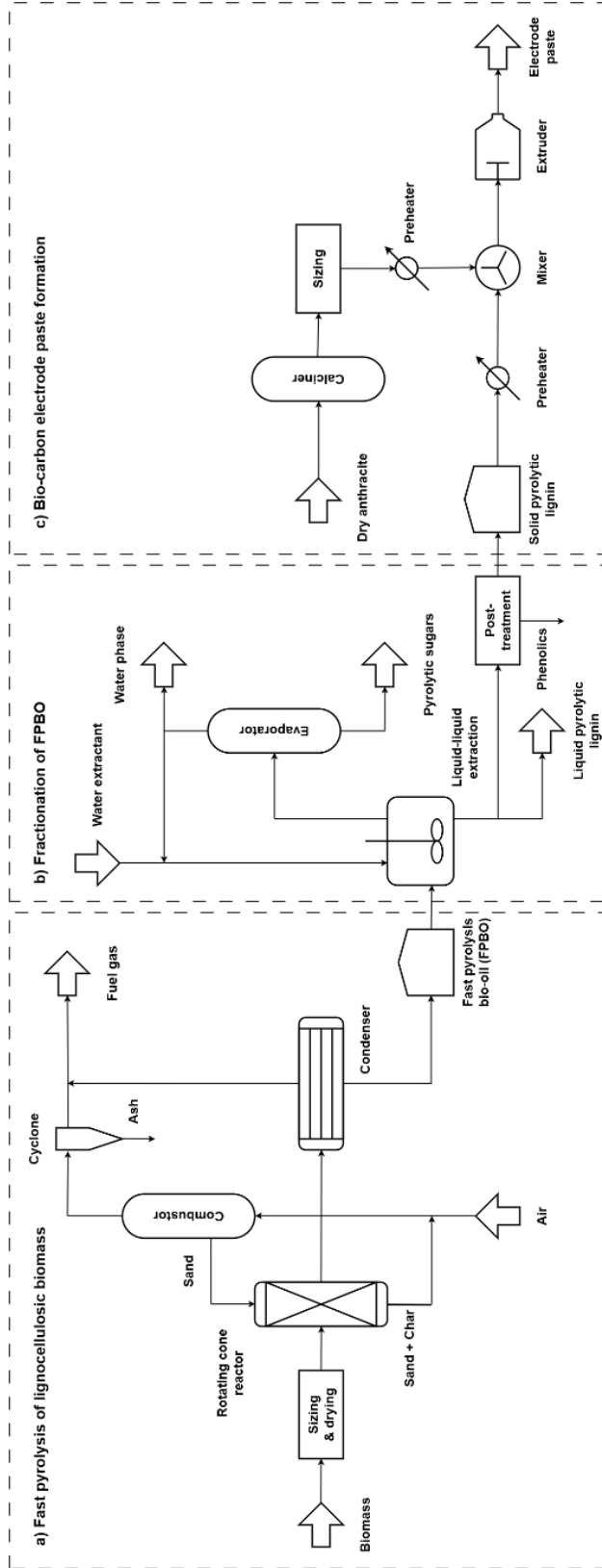


Figure 33. Flowsheet for the bio-carbon electrode formation process from lignocellulosic biomass.